

Received 27 October 2024, accepted 30 December 2024, date of publication 3 January 2025, date of current version 8 January 2025.

Digital Object Identifier 10.1109/ACCESS.2024.3525183

RESEARCH ARTICLE

Automated Defect Detection in Solar Cell Images Using Deep Learning Algorithms

MONTASER ABDELSATTAR^{ID1}, AHMED ABDELMOEY^{ID1},

MOHAMED A. ISMEI^{ID2}, (Senior Member, IEEE), AND AHMED EMAD-ELDEEN³

¹Department of Electrical Engineering, Faculty of Engineering, South Valley University, Qena 83523, Egypt

²Electrical Engineering Department, Faculty of Engineering, King Khalid University, Abha 61411, Saudi Arabia

³Renewable Energy Science and Engineering Department, Faculty of Postgraduate Studies for Advanced Sciences "PSAS," Beni-Suef University, Beni Suef 62511, Egypt

Corresponding author: Montaser Abdelsattar (Montaser.A.Elsattar@eng.svu.edu.eg)

This work was supported by the Deanship of Scientific Research, King Khalid University, through the Large Group Research Project under Grant RGP2/167/45.

ABSTRACT This research study introduces a unique method that makes use of a wide range of deep learning (DL) techniques for automated flaw identification in solar cell images. The research paper investigates how well 24 distinct convolutional neural network (CNN) architectures—Residual network (ResNet), densely connected convolutional networks (DenseNet), visual geometry group (VGG), Inception, mobile network (MobileNet), Xception, SqueezeNet, and AlexNet—classify solar cells into defected and non-defective categories. This study is interesting since it does a thorough assessment of a wide variety of models and concentrates on high-performance architectures and lightweight models that may be used in contexts with limited resources. The research paper performed our studies using a balanced and well-curated dataset of 3,102 images of solar cells with a range of common faults. MobileNetV2 and Xception demonstrated excellent performance in defect identification, with accuracy rates of 99.95% and 99.29% respectively, with minimal validation losses. This study demonstrates the potential of efficient models such as MobileNetV2 for real-world use in solar energy generation. It also provides a detailed comparison of several DL models. The results suggest that the inclusion of these models might significantly enhance quality control systems, offering a reliable and efficient method for detecting flaws in solar cells.

INDEX TERMS Computer vision, defect detection, deep learning, image classification, photovoltaics.

I. INTRODUCTION

Solar energy has become an essential component in the global effort to reduce dependence on fossil fuels and transition to renewable energy alternatives [1]. Solar Photovoltaic (PV) systems are important because they directly convert sunlight into electricity, making use of the plentiful and renewable energy from the sun [2]. The popularity of these systems has increased rapidly due to technological breakthroughs, cost reductions, and growing awareness of the environmental advantages of clean energy generation [3]. The worldwide solar energy industry is growing rapidly, and PV systems are essential in fulfilling the increasing energy needs of both industrialized and developing nations [4]. The growth is motivated by the capacity of solar energy to offer a sustainable

The associate editor coordinating the review of this manuscript and approving it for publication was Ikramullah Lali.

and ecologically sound resolution to the worldwide energy predicament [5].

While PV systems offer numerous savings, but upkeep and inspection of solar cells is one big hiccup in the way. The generation of defects (e.g., micro-cracks, hot spots, the worsening during lifetime) in solar cells is sensitive to a huge number of environmental variables. These defects not only reduce the efficiency of solar cells but also increase maintenance costs due to requiring regular maintenance and possible replacements [6]. Rapid and accurate detection of these failures is important to ensure the longevity and performance of PV systems. Solving these problems at a later date may lead to considerable wastage of energy as well depleted economic viability for solar power projects [7].

There are numerous downsides to conventional ways of spotting flaws in cells, including that manual inspection is intrinsically subjective and thus relies on a human judgement

that is liable to vagaries. This kind of approach also takes an inordinate amount of manual work and time to execute and becomes significantly less effective when applied to scales of large solar farms — this particular form of the approach relies on a person literally walking through the foliage of paneled surfaces [8]. In addition, classical methods based on image processing, while less subjective, often fail to notice the many and varied complex traits of different types of cells' faults, resulting in a considerable amount of overly hasty identifications, both as false positives (FPs) and false negatives (FNs) alike [9].

Electroluminescence (EL) imaging, which is being more widely used for defect identification, provides superior spatial resolution and the capability to detect faults that would otherwise be undetectable. Nevertheless, the interpretation of these images necessitates substantial skill, and the process of manual analysis continues to be expensive and ineffective. The presence of diverse background patterns and the delicate nature of certain flaws pose a significant barrier for automated identification, hence emphasizing the shortcomings of conventional methods [10].

The necessity for automated, precise, and scalable solutions in defect identification is becoming more and more apparent. As the size and quantity of solar farms increase, the limitations of manual and rudimentary image processing techniques become increasingly evident. Deep learning (DL) is a highly effective method for tackling these difficulties, as it is particularly skilled at identifying intricate patterns from extensive datasets. This ability is crucial for accurately detecting defects in solar cells [11]. Through the use of convolutional neural networks (CNNs) and other sophisticated DL architectures, automated systems have the capability to accurately identify problems and categorize them, therefore offering useful insights for maintenance and quality control [12].

Automated tools significantly reduce the time and cost of defect identification that is why they should be used in big solar projects. Moreover, the capacity of DL models to improve detection extends accuracy and efficiency to the utmost by means of ongoing enhancements enabled by the additional data and training necessary for the optimal performance of solar PV systems [13].

DL has transformed the field of image processing, achieving significant success in tasks such as classification, object recognition, and segmentation. DL models differ from typical image processing approaches by relying less on manually designed features and instead learning hierarchical feature representations directly from raw data in an automatic manner. These analyses are enhanced in accuracy and resilience for various tasks [14]. DL techniques have led to major advancements in several fields, including medical imaging. These approaches are successfully used for tasks such as tumor identification, organ segmentation, and illness categorization [15].

DL models have significantly improved the capacity of autonomous vehicles to understand and move through com-

plicated surroundings [16]. They are capable of accurately detecting objects, recognizing traffic signs, and distinguishing various sections of the road. In the field of industrial inspection, DL techniques have been utilized to automate the identification and separation of flaws on different items, therefore improving the efficiency and accuracy of quality control procedures [17].

The significance of using DL in the detection of defects in solar cells derive from the fact that it enables a substantial increase in the levels of accuracy, efficiency, and, more importantly, scalability in using solar cell images. The previously adopted techniques for the detection of defects in solar cells which involve in most cases the manual inspection of the solar cell or rather basic image processing methods are limited in their application to large solar farms. These technologies are primarily subjective and as a result, are highly inefficient [13]. With the use of DL, one can keep training the model on great datasets with labeled images such that they can automatically detect and further classify the defects [18].

Solar energy systems are key to tapping clean, renewable power from the sun and reducing our society's carbon emissions as moving toward a sustainable future. The processing and identification of the PV system faults is necessary to identify errors in PV systems for maintaining solar energy collection efficiency reliability; hence, this is a key frame that takes us on goal about clean low-carbon perspective. Investing in scientific research on fault detection through technologies such as infrared and EL imaging can improve the durability and performance of PV systems, thereby minimizing operational losses and rendering solar energy a more reliable and significant element of the renewable energy sector [19], [20], [21], [22].

The primary objective of this research is to develop and evaluate DL models for the automated detection of defects in solar cell images. The main objective is to detect and categorize flaws in PV modules by utilizing advanced CNNs. The study examines a variety of advanced DL algorithms, such as residual network (ResNet) (ResNet-18, ResNet-34, ResNet-50, ResNet-101, ResNet-152), Densely connected convolutional networks (DenseNet) (DenseNet-121, DenseNet-161, DenseNet-169, DenseNet-201), Visual geometry group (VGG) (VGG-11, VGG-13, VGG-16, VGG-19), Inception (InceptionV1, InceptionV2, InceptionV3, InceptionV4), Mobile network (MobileNet) (MobileNetV1, MobileNetV2, MobileNetV3), Xception, SqueezeNet (SqueezeNet-1.0, SqueezeNet-1.1), and AlexNet. The effectiveness of these models in recognizing faults in solar cell images is assessed using a range of performance criteria, such as accuracy, precision, recall, F1-score, and loss.

This study thoroughly assesses the effectiveness of various DL models in identifying and categorizing flaws in images of solar cells. The study examines the suitability and efficacy of different CNN structures, such as ResNet, DenseNet, VGG, Inception, MobileNet, Xception, SqueezeNet, and AlexNet.

The study seeks to evaluate these models on a collection of solar cell images in order to determine the most efficient architecture for detecting defects. This will provide valuable information about the capabilities and constraints of each model in this particular application. The scope encompasses both binary classification (distinguishing between defective and non-defected) and, when relevant, multi-class classification jobs.

The finding has substantial ramifications for the solar energy sector, specifically in the upkeep and surveillance of PV systems. Implementing automated fault identification in solar cell images can significantly enhance the efficiency of maintenance procedures, hence decreasing the time and expenses linked to manual inspections. Through precise detection of flaws, this research has the potential to result in enhanced maintenance timetables, prolonged durability of solar panels, and enhanced overall energy generation from PV systems. Consequently, this could improve the dependability and cost-efficiency of solar energy as a viable and enduring energy source.

This study adds to the expanding corpus of scholarly research in the fields of DL and renewable energy. The text provides a comprehensive examination of different CNN structures used to address a crucial issue in the solar energy industry. The research examines and assesses various models to gain new insights into the effectiveness of DL algorithms for detecting defects in solar cells. The results can provide guidance for future research endeavors, aiding in the enhancement and optimization of DL methods for comparable applications in different fields.

The research technique comprises various essential stages, commencing with the procurement and preprocessing of a dataset containing images of solar cells. Prior to being divided into training and validation sets, the images undergo pre-processing and normalization. The study entails constructing and instructing numerous DL models, such as ResNet, DenseNet, VGG, Inception, MobileNet, Xception, SqueezeNet, and AlexNet. Every model is trained using the prepared dataset and assessed using a range of performance metrics, such as accuracy, precision, recall, F1-score, and loss. The models' performance is compared to determine the most efficient architecture for detecting defects in solar cell images.

The uniqueness of this study is in its thorough investigation and assessment of a wide variety of advanced DL algorithms specifically used for the automated detection of defects in solar cell images. This research differs from prior studies by doing a comprehensive analysis of many CNN architectures, including as ResNet, DenseNet, VGG, Inception, MobileNet, Xception, SqueezeNet, and AlexNet, instead of solely focusing on one model or a restricted range of architectures. The paper compares these models using several performance indicators to determine the most efficient methods for defect detection. Additionally, it offers new insights into how different architectures handle the intricacies of solar cell images.

The requirement to investigate a wide range of CNN architectures that have demonstrated promise in image classification problems motivated the choice of approaches in this study. With its residual learning structure, ResNet is ideally suited to address the issue of vanishing gradient in deep networks. Because it creates connections between each layer and all layers below it, the DenseNet architecture is selected to promote feature reuse and enhance model efficiency. VGG models are extensively used because of their exceptional performance in a variety of image identification tasks, as well as its recognition for simplicity and efficacy. Because Inception models may extract characteristics at numerous levels, their ability to detect flaws at various levels is investigated. MobileNet is chosen because of its lightweight structure, which makes it ideal for real-time defect detection. MobileNet is primarily designed for mobile and embedded vision applications. Because it makes use of depth-wise separable convolutions, the Xception model—a development of the Inception model—is used. These convolutions preserve performance while effectively lowering the computational burden. SqueezeNet is well known for its small architecture, which results in remarkable speed and model size efficiency. In conclusion, AlexNet is regarded as a trailblazing model in the field of DL, setting the standard for evaluating and contrasting more modern architectural ideas. These algorithms have been selected with the goal of covering a broad range of architectures in order to provide a comprehensive assessment of their capacity to identify flaws in solar cell images.

The detection of defects in PV cells through image processing offers a scalable, rapid and objective replacement for traditional inspection methods. Image processing is able to automatically detect defects in real time instead of using human inspections that are labor-intensive, subjective and often requires a trained operator. This technology supports continuous monitoring of large PV farms to quickly detect small issues, which are often missed with traditional methods. Image processing further improves reliability and efficiency by adding accuracy and consistency to the process mitigating human errors, as well environmental interferes that can reduce the cost of maintenance of PV systems. Compared to conventional methods, it is more economical and versatile, rendering it essential for the maintenance of large-scale solar arrays.

This paper presents a comprehensive and thorough assessment of several CNN architectures in relation to state-of-the-art methods, notwithstanding breakthroughs in automated flaw identification in solar cells utilizing DL. This research specifically evaluates the applicability of both lightweight and high-performance architectures, including MobileNetV2 and Xception, in real-world, resource-constrained settings. This research offers an innovative viewpoint on attaining both elevated precision and computational efficacy. In contrast to other methodologies that often concentrate on one or a few DL architectures, our study systematically compares 24 different models to provide practical insights into

the trade-offs between detection accuracy and processing requirements.

II. LITERATURE REVIEW

Significant progress has been made in the field of automated flaw detection in solar cell images using DL in recent years. This progress has been motivated by the demand for solutions that are efficient, accurate, and scalable. Several distinct DL techniques have been suggested, each offering different approaches and reaching different levels of success.

Table 1 presents an extensive overview of important research on the use of DL for automated flaw detection in solar cell images. **Table 1** showcases a variety of methodologies utilized in different studies, including advanced CNN designs such as EfficientNet-B0 and Xception, as well as hybrid models and segmentation methods. The primary findings of each study, which include advances in accuracy, computing efficiency, and applicability to specific fault kinds, are thoroughly described, demonstrating the advancements and difficulties in this sector. These studies highlight the capacity of DL to improve flaw detection in PV systems, while also pinpointing areas for additional research and enhancement.

The main aim of this study is to create and assess various DL models for automatically detecting faults in photos of solar cells. The ultimate goal is to accurately identify and classify defects while maintaining computational efficiency. The study intends to examine advanced CNNs, including ResNet, DenseNet, VGG, Inception, MobileNet, Xception, SqueezeNet, and AlexNet, to determine the most appropriate architecture for real-time defect identification in PV cells. Ensuring the efficiency and durability of solar panels is very crucial. This research differs from prior studies by examining a wider range of algorithms. It assesses the effectiveness of twenty-four DL models, rather than focussing on a limited number. The models vary in complexity, ranging from basic designs like AlexNet to more intricate networks like ResNet and Inception. The performance of each model is thoroughly evaluated using criteria including as accuracy, precision, recall, F1-score, and computing efficiency. In addition, this study examines sophisticated methodologies. The research aims to conduct a thorough evaluation of these models in order to provide valuable insights into the trade-off between detection accuracy and computational cost. Ultimately, the goal is to identify models that are both highly accurate and computationally efficient, making them suitable for real-time deployment in solar cell defect detection applications.

A. SOILINGEDGE: PV POWER LOSS ESTIMATION USING EDGE DEVICES

Using images from security cameras, a study on the SoilingEdge model suggested a MobileNet-based DL method for estimating power loss in PV systems due to soiling, in 2024 [23]. SoilingEdge intends to evaluate and reduce power loss by considering environmental factors including dust and bird droppings, implemented on many edge plat-

forms including CPUs, FPGAs, VPUs, and EdgeTPUs. The findings revealed that whereas VPU offers cost-effectiveness at a slower processing rate, FPGA shows an ideal balance between cost and inference speed. To improve model interpretability, the study also made use of attention maps, so offering information on model behavior advantageous for engineers as well as researchers.

B. KDBIDET: EFFICIENT PV HOT-SPOT DETECTION USING KNOWLEDGE DISTILLATION

In 2024, Hao et al. KDBiDet, proposed by Liu et al., is a knowledge distillation-based model with bi-branch teacher-student framework for the practical problem of PV hot-spot detection [24]. Method: KDBiDet utilizes you only look once X (YOLOX) as a lightweight student network with HorNet-based teacher for better feature representation, and multi-scale features are integrated through bilateral multi-scale adaptive fusion (BiMAF) module in conjunction with Spatial-Channel transformer (SCT) based prediction head to encourage cross-scale interaction. The AP50 results of KDBiDet for the 13 algorithms ensure a fast and accurate detection of hot-spot faults in PV systems.

C. ViT MODEL FOR FAULT DETECTION IN PV MODULES

Using thermographic IR images and integrating ViT Neural Network, Ramadan et al. developed a unique fault detection method in PV modules in 2024 to attain better performance while processing these early identification tasks related to the faults [25]. The framework includes three primary stages: image preprocessing using unsharp masking for edge enhancement, data augmentation to manage class imbalance and extracting high-level features through ViT. The model was tested on the Infrared Solar Modules dataset and it achieved 98.23% binary classification (fault/no-fault) accuracy, as well as 96.19% across eleven PV fault types which represent significantly better performance over other DL models. The marketing is there to convince you, as a professional researcher or practitioner for early fault diagnosis in PV modules prior to the updated literature signal: it took just three months from accepting this work.

D. INFRARED-VISIBLE IMAGE FUSION FOR PV HOT SPOT DETECTION

In 2024, a PV fault detection model combining infrared-visible image fusion and generative adversarial network based (GAN-based) augmentation is proposed to detect hotspot faults for an extreme weather condition [26]. The main separation strategy described is based on cosine distance Pseudo-Label cross-entropy (CDPC) to ensure that image pairs are of high quality and boost detection accuracy and efficiency. The study achieved 93.7% fine-grained fault detection accuracy with an improved data quality and reduced by 30 script requirements of training data, leading to a dual economic (trained time) and ecological gain (less emission).

TABLE 1. Summary of key studies on automated defect detection in solar cell images using DL.

Reference	YEAR	TECHNIQUE USED	STUDY DESCRIPTION	MAJOR FINDINGS
[23]	2024	MobileNet-based DL model for edge devices.	Created SoilingEdge, a methodology for quantifying PV power loss due to soiling, implemented on central processing units (CPUs), Field programmable gate arrays (FPGAs), Vision processing units (VPUs), and edge tensor processing units (EdgeTPUs).	Whereas VPU is the most economical with slower performance, FPGA provides a compromise between cost and performance.
[24]	2024	Knowledge distillation with bi-branch collaborative training.	Enhanced the efficiency of PV hot-spot detection by establishing a teacher-student structure that employs YOLOX as a student model. This structure is further enhanced by a contextual transformer and multi-scale feature fusion.	Attained an AP50 score of 82.2%, indicating proficient and fast multi-scale hot-spot identification across varied situations.
[25]	2024	Vision transformer (ViT) model with image preprocessing and data augmentation.	Applied ViT with improved preprocessing and class balancing for accuracy to early PV fault detection on thermographic infrared radiation (IR) images.	Better than traditional DL models at detecting multiple PV fault types with 98.23% classification accuracy.
[26]	2024	GAN-based infrared-visible image fusion.	Developed a system for detecting PV hot spots using fusion and CDPC algorithms.	Improved data quality and training efficiency with 93.7% accuracy.
[27]	2024	CNN-based classification with GoogleNet, SqueezeNet, and LwNet.	used CNN models, utilizing transfer learning (TL) and dataset augmentation, to categorize PV faults from EL images.	Over GoogleNet and SqueezeNet, LwNet was most accurate (96.2%) and efficient.
[28]	2024	TL with depth reduction (TLDR-CNN) and gradient-weighted class activation mapping (Grad-CAM).	To optimize CNNs for PV defect classification on infrared images, multi-scale feature extraction and TL were used.	The optimized CNN model enhanced classification accuracy, efficiency, interpretability, and fault localization precision.
[29]	2024	Residual learning with YOLOv4 and UAV-based image analysis.	Engineered a UAV-based YOLOv4 model using residual learning for fault location in PV systems.	high accuracy, effective defect localization, and light computing effort.
[30]	2024	Image processing with mathematical morphology and A* path planning.	Using image enhancement and binarization techniques, a UAV-assisted grime detection method for PV panels was developed.	The technology greatly improves detection efficiency, lowers maintenance costs, and increases PV operating dependability.
[31]	2024	Improved YOLOv8-GD model (DW-Conv, GSConv, BiFPN).	A lightweight model has been developed to detect defects in PV modules. The model has been validated using EL datasets.	Improved accuracy by 4.2%-5.7%, reduced model size by 16.7%.
[32]	2024	CNN-based detector with EfficientNet-B0, CLAHE, Grad-CAM, and focal loss.	A new approach is introduced for accurately detecting defects in solar cells using EL images, which improves contrast and integrates global information modeling.	The model achieved an accuracy of 97.81%, surpassing state-of-the-art methods in multiple metrics, including precision, recall, F1-score, and MCC.
[33]	2023	Custom CNN.	Presented a CNN method for identifying surface flaws on solar cell busbars, with a specific emphasis on intricate texture backgrounds.	Achieved 85.8% accuracy in defect recognition, improving detection effectiveness in solar cell manufacturing.
[34]	2023	Improved G-SSD, GhostNet.	Created an algorithm utilizing the enhanced G-SSD network to identify defects in solar cells, specifically designed to perform well on small-sized targets.	Improved mAP by 0.68% and reduced computational costs.
[35]	2023	TL-ResNet50.	Implemented TL using the ResNet50 architecture to detect defects on steel surfaces. Improved the model's performance by applying learning rate decay and utilizing the Adam optimizer.	Achieved 99.4% accuracy on the testing set.
[36]	2023	InceptionV3, EfficientNetB3, U-Net.	Employed CNN-classifier models and U-Net for the purpose of detecting and segmenting concrete defects, such as cracks and spalling.	InceptionV3 achieved 91.98% accuracy for defects classification.
[37]	2022	DL-based segmentation models (DeepLabV3+, FPN, U-Net) using thermal images from UAVs.	Identification of faulty solar panels in expansive solar farms with thermal images obtained by UAVs and a range of sophisticated DL algorithms.	U-Net achieved the highest performance with an IoU of 86% and a dice coefficient of 94%, proving the models effective for fault detection.
[38]	2022	ResNet152-Xception, Coordinate Attention Mechanism.	A novel DL model combining ResNet152 and Xception for PV cell defect detection using EL images.	Achieved 96.17% accuracy for binary classification and 92.13% for multi-classification tasks.
[39]	2022	AlexNet, SENet, ResNet, Xception.	Applied DL networks to classify defects in solar PV cells using EL images.	Achieved high accuracy, with Xception model performing best.
[40]	2022	DFB CNN.	Proposed a DFB method combined with machine learning for defect detection in solar cells.	Achieved 98.15% and 95.35% accuracy for binary and multi-class tasks, respectively.
[41]	2021	SqueezeNet, MobileNet, InceptionV3.	Compared multiple CNN architectures for automated defect detection in PV cells.	Found MobileNet-SSD to be highly efficient in defect detection.

TABLE 1. (Continued.) Summary of key studies on automated defect detection in solar cell images using DL.

[42]	2020	AlexNet.	Utilized TL with AlexNet to identify surface flaws on PV solar panels, demonstrating the efficacy of DL in classifying faults.	Achieved promising performance in detecting various surface defects on solar panels.
[43]	2020	AlexNet, InceptionV3, Xception.	Applied TL and deep CNNs for defect detection in PV panels using EL images.	Achieved 91.399% accuracy using the Xception model.
[44]	2019	CNN.	Suggested a DL approach to identify and classify fault patterns in large-scale PV farms using aerial images captured by drones.	The model significantly improved the efficiency and accuracy of asset inspection and health assessment for large-scale PV farms.
[45]	2019	Faster-RCNN, FPN, GA-RPN.	Created a system for identifying surface defects in solar cells using the Faster-RCNN algorithm, which was further refined with the addition of FPN and guided anchoring region proposal network (GA-RPN) to enhance both accuracy and speed.	Achieved a mAP of 94.62% and significantly increased detection speed, making it suitable for industrial production.
[46]	2019	SEF-CNN.	Suggested an innovative approach that integrates conventional filters with CNN to identify crack defects in solar cells, hence minimizing the occurrence of false detections caused by background interference.	Improved the robustness and accuracy of crack detection in EL images.
[47]	2019	U-Net, Dilated Convolution, Global Attention.	Created an enhanced U-Net model using dilated convolution and global attention to accurately identify defects in PV EL images.	The model achieved a mean IoU of 0.6477 and a pixel accuracy of 0.9738, surpassing other state-of-the-art methods.

E. CNN-BASED CLASSIFICATION OF PV DEFECTS IN EL IMAGES

A CNN-based TL method for defect classification in EL images of PV modules was proposed with use of GoogleNet, SqueezeNet and newly developed lightweight customized lightweight network (LwNet) model in 2024 [27]. The models were trained on the augmented ELPV dataset and tested in 4/8-class classification using enhanced data. In the end, LwNet obtained an accuracy of 96.2 % which is much better than GoogleNet and SqueezeNet are highly efficient in terms of classification performance so that it can be used as a solution for quick and accurate detection of PV defects.

F. TL AND DEPTH-REDUCED CNN FOR PV FAULT DETECTION

Emphasizing model efficiency and interpretability, a paper presented a transfer learning-based depth reduction method (TLDR-CNN) for classifying PV module faults from infrared images in 2024 [28]. The model replaced convolutional layers using a multi-scale feature extraction (MSFE) module based on VGG16, so lowering complexity and improving performance. With a 6.89% rise in F1 score and a 1.01% increase in matthews correlation coefficient (MCC), experimental data showed notable gains. For interpretability, Grad-CAM was used to confirm that the altered model efficiently focused on important fault areas, so maximizing feature extraction and accuracy.

G. RESIDUAL LEARNING FOR PV FAULT DETECTION

In 2024, Zhang et al. introduced a residual learning-enhanced YOLOv4 model for the efficient identification and localization of faults in low-voltage PV modules, utilizing UAV-based image acquisition. The model improves accuracy and speed in P0V fault localization tasks by incorporating multi-scale spatial pyramid fusion and Complete-IOU loss. Comparative analyses of diverse PV plant scenarios demonstrate the

model's exceptional adaptability, attaining enhanced fault localization while minimizing memory and computational requirements, thereby surpassing conventional models in operational efficiency and accuracy. The research illustrates the model's capability for real-time PV monitoring, advantageous for extensive operations and maintenance applications [29].

H. IMAGE PROCESSING-BASED PV DIRT DETECTION METHOD

In 2024, Xiang et al. [30] presented an image processing technique for identifying contaminants on PV cell surfaces, targeting efficiency reductions caused by ash and debris accumulation. The research employs mathematical morphology techniques, such as image enhancement, sharpening, and binarization, to enhance target recognition accuracy across diverse lighting conditions. Furthermore, histogram equalization improves image contrast, facilitating more accurate detection of soiled regions. An optimized A* path planning algorithm was integrated to enhance UAV detection efficiency, thereby reducing time and resource consumption while improving the maintenance efficiency and cost-effectiveness of PV systems.

I. IMPROVED YOLOv8-GRADIENT DESCENT (YOLOv8-GD) MODEL FOR PV MODULE DEFECT DETECTION

In 2024, Cao et al. [31] proposed an improved YOLOv8-GD model that introducing depthwise convolution (DW-Conv), Ghost convolution (GSConv) and bi-directional feature pyramid network (BiFPN). These modifications enhance fault detection in PV modules that is conducted through EL images. The extensive validation on multiple datasets showed that the proposed model enhances the performance in terms of accuracy by 4.2% – 5.7% and reduces its size by 16.7%. The researchers conclude that lightweight models can exhibit the high level of accuracy while reducing the burden of

computing, which allows for using these tools for real-time applications.

J. CNN-BASED DETECTOR WITH EFFICIENTNET-B0 AND CLAHE

In 2024, Liu et al. [32] developed a CNN detector using EfficientNet-B0, CLAHE, Grad-CAM, and focal loss techniques. The main finding of this study is that the authors designed a detector that can accurately detect solar cell flaws using EL images. A unique method enhances information distinction and representation. The accuracy rate of 97.81% is exceptional and better than the most advanced techniques in precision, recall, F1-score, and MCC. Overall, the study shows that contrast improvement and global information improve defect identification.

K. CUSTOM CNN FOR SOLAR CELL BUSBARS SURFACE DEFECT DETECTION

In 2023, Balcioglu et al. [33] introduced a specialized CNN designed to identify surface flaws on solar cell busbars. The network specifically emphasizes its ability to handle intricate texture backdrops. The technique attained an accuracy of 85.8%, indicating an enhancement in the efficacy of detecting issues during the solar cell manufacturing process. This study highlights the significance of customized CNN architectures in tackling unique obstacles, such as intricate background textures, in defect detection.

L. IMPROVED GHOST SINGLE SHOT DETECTOR (G-SSD) NETWORK AND GHOSTNET FOR SMALL-SCALE TARGET DETECTION

Xu [34] in 2023 introduced an improved G-SSD network optimized for small-scale target detection in solar cells, incorporating GhostNet to enhance computational efficiency. The proposed technique enhanced the Mean Average Precision (mAP) by 0.68% while simultaneously reducing computational expenses, hence showcasing the efficacy of focused network enhancements in optimizing detection performance.

M. TRANSFER LEARNING (TL) WITH ResNet50 FOR STEEL SURFACE DEFECT DETECTION

Zhang et al. [35] explored TL with ResNet50 for detecting steel surface defects, applying techniques such as learning rate decay and the adaptive moment estimation (Adam) optimizer to enhance model performance. Their methodology demonstrated an exceptional level of precision, reaching 99.4% accuracy when applied to the testing set. This highlights the potential of TL in enhancing defect detection in similar fields, such as solar cell flaw detection.

N. MULTI-MODEL APPROACH USING INCEPTIONV3, EFFICIENTNETB3, AND U-SHAPED CONVOLUTIONAL NEURAL NETWORK (U-NET)

In 2023, Arafin et al. [36] utilized CNN-classifier models and U-Net to identify and separate concrete problems, such as cracks and spalling. The analysis revealed that InceptionV3

attained a classification accuracy of 91.98%. The utilization of DL models in both classification and segmentation tasks demonstrates their adaptability, emphasizing its potential in detecting defects in solar cells.

O. DL-BASED SEGMENTATION MODELS USING THERMAL IMAGES FROM UNMANNED AERIAL VEHICLES (UAVs)

In 2022, Jumaboev et al. [37] utilized advanced DL-based segmentation models, including DeepLabV3+, Feature pyramid network (FPN), and U-Net, to identify faulty solar panels in extensive plantations. This was achieved by analyzing thermal images obtained from UAVs. Out of all the models that were tested, U-Net had the most superior performance, achieving an intersection over union (IoU) score of 86% and a dice coefficient of 94%. This study showcases the efficacy of DL in the processing and analysis of thermal images for the detection of defects in large-scale solar panels.

P. ResNet152-Xception HYBRID MODEL WITH COORDINATE ATTENTION MECHANISM

In 2022, Wang et al. [38] proposed a hybrid model that integrates ResNet152 and Xception with a Coordinate Attention Mechanism to detect defects in solar cells using EL images. The model achieved a precision of 96.17% for binary classification and 92.13% for multi-classification tasks. This research emphasizes the benefits of combining hybrid models and attention mechanisms to enhance the accuracy of defect detection.

Q. COMPARISON OF DL NETWORKS FOR SOLAR PV CELL DEFECT CLASSIFICATION

Tella et al. [39] in 2022 conducted a comparative study on various DL networks, several DL models, such as AlexNet, Squeeze-and-Excitation network (SENet), ResNet, and Xception, are utilized to classify faults in solar PV cells based on EL images. The Xception model demonstrated superior performance compared to other models, attaining the maximum level of accuracy. This confirms its efficacy in classifying defects in solar cells.

R. DEEP FEATURE-BASED (DFB) CNN FOR PV MODULE DEFECT DETECTION

Al-Waisy et al. [40] presented a DFB CNN integrated with machine learning in 2022 for the purpose of detecting defects in solar cells. Their methodology resulted in achieving 98.15% and 95.35% accuracy for binary and multi-class tasks, respectively. This study emphasizes the capacity of deep feature extraction to enhance defect detection performance in solar modules.

S. COMPARATIVE ANALYSIS OF CNN ARCHITECTURES FOR AUTOMATED DEFECT DETECTION

In 2021, Katiyar et al. [41] conducted a comparative analysis of various CNN designs, such as SqueezeNet, MobileNet, and InceptionV3, to evaluate their effectiveness in detecting defects in PV cells. The study determined

that MobileNet-SSD is remarkably efficient, achieving a harmonious equilibrium between accuracy and computing efficiency. This comparison highlights the significance of choosing a model based on the specific requirements of the application when it comes to defect identification.

T. TL WITH ALEXNET FOR PV SOLAR PANEL SURFACE DEFECT DETECTION

Zyout and Oatawneh [42] in 2020 utilized TL with AlexNet to identify surface flaws on PV solar panels. Their research demonstrated the capabilities of DL, specifically AlexNet, in classifying defects, yielding encouraging outcomes in the identification of different surface flaws.

U. TL AND CNNS FOR PV PANEL DEFECT DETECTION USING EL IMAGES

In 2020, Su et al. [43] utilized TL and deep CNNs such as AlexNet, Inception V3, and Xception to detect defects in PV panels using EL images. The Xception model attained a peak accuracy of 91.399%, showcasing its efficacy in addressing intricate fault detection tasks in PV panels.

V. DL FOR DEFECT PATTERN RECOGNITION IN AERIAL IMAGES OF PV FARMS

In 2019, Li et al. [44] introduced a system based on DL to recognize flaw patterns in large-scale PV farms using aerial images captured by drones. The approach greatly enhanced the efficiency and precision of asset inspection and health evaluation, rendering it a valuable tool for managing large-scale PV farms.

W. FASTER-RCNN WITH FPN AND GA-RPN FOR SOLAR CELL SURFACE DEFECT DETECTION

In 2019, Liu et al. [45] created a surface defect detection system using Faster-Region-based convolutional neural network (Faster-RCNN). They improved the accuracy and speed of the system by using FPN and GA-RPN. The system attained a mAP of 94.62% and shown a substantial enhancement in detection speed, hence showcasing its appropriateness for deployment in industrial production settings.

X. SEF-CNN FOR CRACK DETECTION IN EL IMAGES

Chen et al. [46] in 2019 introduced a novel model called steerable evidence filter convolutional neural network (SEF-CNN). This approach utilizes a combination of conventional filters and CNN to identify cracks in solar cells. By implementing this method, the occurrence of false detections resulting from background interference was minimized, leading to enhanced reliability and precision in identifying cracks in EL images.

Y. U-NET WITH DILATED CONVOLUTION AND GLOBAL ATTENTION FOR DEFECT SEGMENTATION

In 2019, Rahman et al. [47] created an enhanced U-Net framework that incorporates dilated convolution and global attention to accurately identify defects in PV EL images. The

model attained a mean IoU of 0.6477 and a pixel accuracy of 0.9738, surpassing previous cutting-edge techniques in defect segmentation.

III. METHODOLOGY

A. DATA PRESENTATION

Table 2 displays the distribution of defective and non-defective solar cell images in the dataset utilized for training and assessing DL models. The collection consists of 3,102 images, of which 1,570 are categorized as defective and 1,532 are categorized as non-defective. A number of these datasets were gathered from multiple sources, as referenced in [48], [49], and [50], while others were acquired from our additional sources, demonstrating a significant degree of balance. The dataset was collected from several sources and demonstrates a significant degree of equilibrium. The data has been normalized to ensure consistency and improve model training. Additionally, it has undergone preprocessing to achieve a uniform size of 244 × 244 pixels. In order to evaluate the effectiveness of different DL algorithms, such as ResNet, DenseNet, VGG, Inception, MobileNet, Xception, SqueezeNet, and AlexNet, the dataset is divided into training and validation sets with a ratio of 80-20.

TABLE 2. Distribution of defected and non-defected solar cell images in the dataset.

Type	Count
Defected	1570
Non-Defected	1532
Total	3102

Figure 1 displays instances of flaws in solar cells, presenting a collection of ten cells without defects (top two rows) and ten cells with problems (bottom two rows) from the dataset utilized in this study. The cells that are not faulty are highlighted in green, emphasizing their normal structural integrity and absence of observable abnormalities. Conversely, the faulty cells are marked in red to signify the existence of diverse abnormalities, such as fractures, discolorations, and other physical imperfections. The resolution of each image is set at 224 × 224 pixels to ensure uniformity and enable thorough study of the cell surfaces. The visual representation plays a vital role in the automated defect identification process by allowing the algorithm to distinguish between normal and defective cells based on clear visual characteristics. The graphic illustrates samples that offer a distinct comparative understanding of the visual features that differentiate faulty solar cells from their non-faulty counterparts. This emphasizes the dataset's efficacy in training and validation defect detection methods. In the images presented in **Figure 1**, the horizontal and vertical axes denote pixel dimensions. The axes span from 0 to 224 pixels, aligning with the predefined dimensions of 224 × 224 pixels employed in this study, so ensuring homogeneity across all images for consistent input to the DL models.

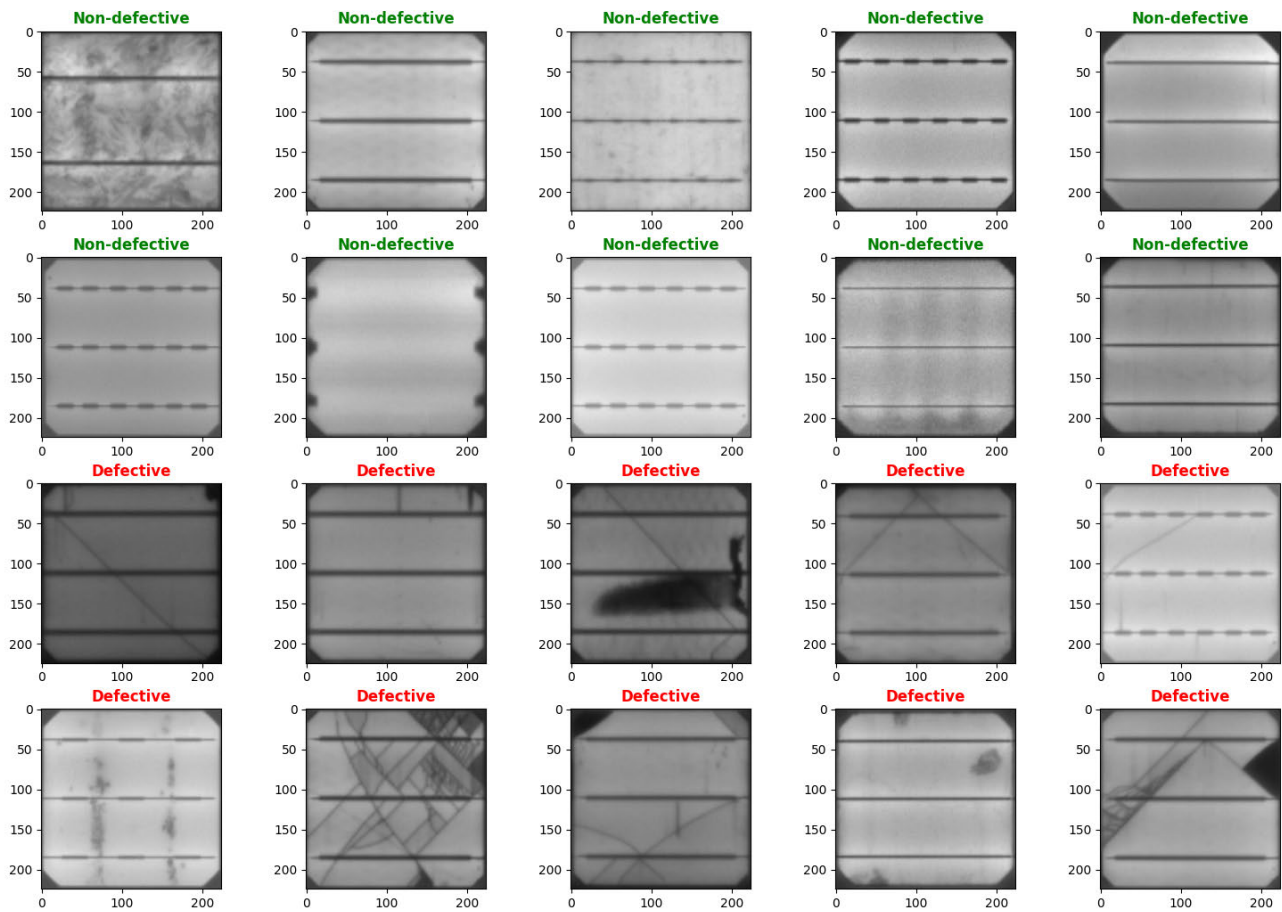


FIGURE 1. Representative Samples of Defective and Non-Defective Solar Cells from the Dataset.

B. DL ALGORITHMS

Table 3 provides a comprehensive overview of the essential parameters included in the solar cell image categorization model. The images were uniformly adjusted to a height and width of 244 pixels each in order to maintain consistency throughout the collection. During the data division process, a random seed value of 42 was utilized to ensure reproducibility. With a batch size of 16, the model was trained for 25 epochs, which allowed it to update its weights after processing every 16 samples. The model's performance in binary classification tasks was assessed using the binary cross-entropy loss function, and the Adam optimizer was chosen for its effective optimization capabilities. The validation loss was continuously monitored in order to implement the early stopping method. In order to avoid overfitting, a minimum change of 0.01 was necessary and a patience threshold of three epochs was established. To ensure optimal performance, the model was further configured to take the most accurate weights from the epoch with the lowest validation loss.

Table 4 displays a thorough comparison of different DL methods utilized for the automated detection of defects in images of solar cells. **Table 4** contains essential metrics, including parameter count, model size, computational com-

plexity, feature handling capabilities, and interpretability [51], [52], [53], [54], [55], [56], [57], [58]. The ResNet models, which include ResNet-18 to ResNet-152, exhibit robust feature processing capabilities with different degrees of complexity and interpretability. The DenseNet family, renowned for its dense connection patterns, has exceptional proficiency in feature manipulation, but at the expense of interpretability. VGG models possess a large number of parameters, which results in weak feature handling capabilities and low interpretability. Inception models provide a harmonious mix between complexity and feature management, rendering them well-suited for efficient computation. MobileNet variations are distinguished by their low complexity and good interpretability, making them well-suited for deployment on devices with limited resources. The Xception and SqueezeNet models offer a balance between feature handling and model size, with SqueezeNet being particularly efficient in terms of the number of parameters it requires. **Table 4** summarizes the strengths and weaknesses of these algorithms, guiding algorithm selection for solar cell defect detection.

The automatic flaw detection process in solar cell images, depicted in **Figure 2**, is carefully organized into multiple crucial phases, each playing a role in the overall research

TABLE 3. Parameters used in the solar cell image classification model.

Parameter	Value	Description
'img_height'	244	Image height used for resizing during preprocessing
'img_width'	244	Image width used for resizing during preprocessing
'random_state'	42	Random seed used for data splitting to ensure reproducibility
'batch_size'	16	Number of samples per gradient update during model training
'epochs'	25	Number of iterations over the entire dataset for training the model
'optimizer'	'adam'	Optimization algorithm used for training the model
'loss'	'binary_crossentropy'	Loss function used for binary classification
'monitor'	'val_loss'	Metric monitored during training for early stopping
'min_delta'	0.01	The smallest change in the monitored metric required to be considered an improvement.
'patience'	3	The number of consecutive epochs without improvement before early stopping occurs.
'restore_best_weights'	True	Whether to restore model weights from the epoch with the best value of the monitored quantity

TABLE 4. Comparison of DL algorithms for automated defect detection in solar cell images.

Algorithm	Parameters	Size (MB)	Complexity	Feature Handling	Interpretability
ResNet-18	11.7M	44	Moderate	Strong	Moderate
ResNet-34	21.8M	85	Moderate	Strong	Moderate
ResNet-50	25.6M	98	High	Strong	Moderate
ResNet-101	44.5M	171	High	Strong	Low
ResNet-152	60.2M	230	High	Strong	Low
DenseNet-121	8.0M	33	High	Very Strong	Low
DenseNet-161	28.7M	120	High	Very Strong	Low
DenseNet-169	14.3M	62	High	Very Strong	Low
DenseNet-201	20.2M	88	High	Very Strong	Low
VGG-11	132.9M	507	High	Moderate	Low
VGG-13	133.0M	508	High	Moderate	Low
VGG-16	138.4M	528	High	Moderate	Low
VGG-19	143.7M	548	High	Moderate	Low
InceptionV1	5.6M	21	Moderate	Strong	Moderate
InceptionV2	11.2M	42	Moderate	Strong	Moderate
InceptionV3	23.8M	89	High	Strong	Moderate
InceptionV4	41.2M	153	High	Strong	Moderate
MobileNetV1	4.2M	17	Low	Moderate	High
MobileNetV2	3.5M	14	Low	Moderate	High
MobileNetV3	2.5M	10	Low	Moderate	High
Xception	22.9M	88	High	Very Strong	Moderate
SqueezeNet-1.0	1.2M	4.6	Low	Moderate	High
SqueezeNet-1.1	1.2M	4.8	Low	Moderate	High
AlexNet	61M	240	High	Moderate	Moderate

workflow. The procedure commences with data preprocessing, in which the data is initially extracted from many sources, including images of both faulty and non-faulty solar cells. The images undergo a vital normalization step to standardize their pixel values, usually by scaling them within the range of 0 to 1. This step guarantees the stability and efficiency of the training process, enabling the model to learn with optimal effectiveness. After normalizing the data, it is divided into training and validation sets. This is an important step to assess the model's performance on new, unseen data and prevent overfitting. This division is essential for ensuring a strong validation of the model's predicting ability.

After the data has been prepared, the technique moves on to the phase of selecting the algorithm. At this point, a choice is made about the DL algorithm to use from a predeter-

mined selection, which includes ResNet, DenseNet, VGG, Inception, MobileNet, Xception, SqueezeNet, and AlexNet. The selection is determined by the specific requirements of the experiment, which may include the necessity for precise calculations, architectural preferences, or both. The choice of the algorithm is essential, as it directly influences the performance of the model and the results of the experiment.

Once the algorithm has been selected, the subsequent stage involves advancing to the phase of model development. In this scenario, the model is built by considering the structure of the selected approach, which involves defining the layers, activation functions, and configuring the model with an appropriate optimizer and loss function. After constructing the model, the training phase begins, in which the model is exposed to the training dataset. At this stage, the model develops the

capacity to differentiate between defective and non-defective images by adjusting its internal parameters through the process of backpropagation and optimization. After the training is finished, the model's performance is evaluated by using the validation set. This evaluation produces essential indicators, including accuracy and loss, which offer significant insights into the model's learning effectiveness and its ability to generalize to new data.

The last stage of the process is results visualization, which aims to thoroughly analyses and present the model's performance. At first, the training and validation metrics are graphed to visually represent the accuracy and loss patterns over the training epochs. This visualization facilitates the detection of potential challenges, such as overfitting or under fitting. Subsequently, the model's predictions on the validation set are presented visually, allowing for a qualitative assessment of the model's performance. Subsequently, a thorough classification report is generated, encompassing accurate measurements such as precision, recall, F1-score, and support for every class (both defined and non-defined). These measures together offer a comprehensive evaluation of the model's performance. In the end, a confusion matrix is created, which gives a thorough evaluation of the model's skills and constraints, particularly in its ability to distinguish between distinct types of images.

The flowchart demonstrates a methodical and structured process for automatically detecting defects in solar cells. The study is meticulously designed to facilitate a methodical and dependable evaluation of the DL algorithms employed. This encompasses all facets, including data preprocessing and visualizing the outcomes. Ultimately, this process yields significant findings regarding their performance and identifies potential avenues for improvement.

C. EVALUATION METRICS

This research paper utilized a wide range of evaluation measures to accurately evaluate the effectiveness of several DL models in detecting defects in solar cell images. The chosen measures comprise Precision, Recall, F1-Score, Support, Accuracy, Loss, Validation Accuracy, and Validation Loss as references in [59], [60], [61], and [62]. Every indicator offers distinct perspectives on the model's efficiency in detecting errors, guaranteeing a strong evaluation framework.

Precision is calculated by dividing the number of correctly predicted positive observations by the total number of predicted positive observations. When the cost of FPs is significant, it is essential to validate the accuracy of the model in identifying defective solar cells without incorrectly labelling non-defective ones. **Equation (1)** provides the formula for Precision. Here, True positives (TPs) represents the number of correctly identified defected images, and FP is the number of non-defected images incorrectly classified as defected.

Recall, also known as Sensitivity or TP Rate, is the ratio of correctly predicted positive observations to the total number of actual positive observations. This metric is crucial

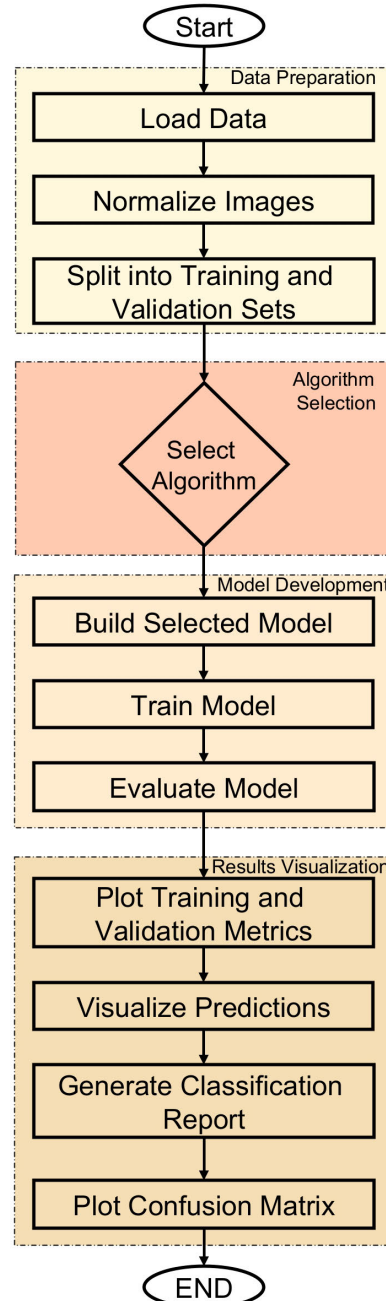


FIGURE 2. Flowchart of the Methodology for Automated Defect Detection in Solar Cell Images Using DL Algorithms.

in situations where the consequences of FNs are significant, guaranteeing that the model accurately detects all occurrences of defective solar cells, hence reducing the likelihood of missing any flaws. The calculation of recall is determined according to (2), where FN represents the number of defected images that were incorrectly classified as non-defected.

The F1-Score is a mathematical average that combines Precision and Recall, resulting in a single metric that effectively balances the trade-offs between these two measures. It is especially beneficial in situations where the dataset is

imbalanced, as it gives equal importance to both Precision and Recall, allowing for a full evaluation of the model's performance. The F1-Score is calculated using (3).

Support is a metric that quantifies the frequency of each class in the dataset. The contextual information provided includes the sample size used to construct metrics such as Precision, Recall, and F1-Score. This analysis offers valuable information on the distribution of the dataset and the dependency of the calculated measures. Support is not quantified mathematically, but instead is determined by tallying the frequency of occurrences in each category. Accuracy is the proportion of accurately predicted observations to the total number of observations. Although it offers a comprehensive indication of the model's accuracy in classifying images, this metric might be deceptive in datasets with uneven distribution, necessitating the evaluation of additional metrics in conjunction. **Equation (4)** provides the formula for calculating Accuracy. In this equation, True negatives (TN) is the number of non-defected images correctly classified as non-defected.

Loss measures the difference between the predicted output and the actual output. This study used binary cross-entropy as the loss function, which is widely used for binary classification tasks. Minimizing the loss during model training is essential for accurately evaluating the model's learning progress. **Equation (5)** provides the formula for calculating loss. Here, N is the total number of samples, y_i represents the actual label for the i -th sample (1 for defected, 0 for non-defected), and p_i denotes the anticipated probability that the i -th sample is defected.

Validation Accuracy is a metric that measures the accuracy of a model on a validation set, which is a collection of data that the model has not been exposed to during training. This statistic serves to assess the model's performance on data that has not been previously observed, providing a means to identify overfitting. The validation accuracy is calculated using the same formula as the accuracy, as indicated in (4), but it is applied to the validation set. Validation Loss is a metric that is similar to Loss, but it is specifically calculated using the validation dataset. Monitoring overfitting is critical, as it is indicated by an increasing Validation Loss and a decreasing training loss. Loss often signifies that the model is beginning to memories the training data instead of extrapolating from it. The computation for Validation Loss is identical to that of Loss, as indicated in (5), but it is specifically applied to the validation data.

$$\text{Precision} = \frac{TP}{TP + FP} \quad (1)$$

$$\text{Recall} = \frac{TP}{TP + FN} \quad (2)$$

$$F1 - Score = 2 \times \frac{\text{Precision} \times \text{Recall}}{\text{Precision} + \text{Recall}} \quad (3)$$

$$\text{Accuracy} = \frac{TP + TN}{TP + TN + FP + FN} \quad (4)$$

$$\text{Loss} = -\frac{1}{N} \sum_{i=1}^N [y_i \log(p_i) + (1 - y_i) \log(1 - p_i)] \quad (5)$$

The equations presented here establish a mathematical basis for evaluating the DL models employed in this study. This ensures a comprehensive and precise evaluation of their effectiveness in detecting flaws in solar cell images.

IV. RESULTS AND DISCUSSION

This section focusses on the outcomes and analysis of our research about the relative effectiveness of DL models in identifying defects in images of solar cells. The research paper investigates the effectiveness of chosen models in detecting faults by conducting a thorough assessment that includes evaluating accuracy, loss metrics, and confusion matrices. The models selected are the most high-performing versions from several architectural families, especially chosen to demonstrate the range of capabilities in modern DL technology. The following analysis offers a comprehensive evaluation of the performance of each model, highlighting their advantages and disadvantages, and providing guidance for selecting the most suitable model for practical use in quality control processes in the solar cell manufacturing business.

Table 5 displays a comprehensive examination of DL models employed for the automated identification of flaws in solar cell images. It emphasizes their effectiveness in terms of different measurements, including accuracy, loss, validation accuracy, and validation loss. **Table 5** is arranged in ascending order of performance within each family of models. Out all the architectures assessed, MobileNetV2 distinguishes itself with the maximum accuracy of 99.95% and a minimal loss of 0.0075. Furthermore, it demonstrated an impressive validation accuracy of 99.84% and a validation loss of 0.0068, which signifies exceptional performance and resilience in identifying flaws in previously overlooked data. Xception and MobileNetV1 shown outstanding performance. Xception achieved an accuracy of 99.29%, a validation accuracy of 99.03%, and a validation loss of 0.0299. On the other hand, MobileNetV1 achieved an accuracy of 99.42%, a validation accuracy of 99.19%, and a validation loss of 0.0174. These results demonstrate their efficacy in managing fault detection tasks. On the other hand, models such as SqueezeNet-1.0 and SqueezeNet-1.1 exhibited inferior performance, as seen by their accuracy of 47.71%, validation accuracy of 47.34%, and validation loss of 0.6941. These results indicate that these models have limitations when it comes to detecting defects. The evaluation presented in **Table 5** offers significant insights into the strengths and drawbacks of various DL architectures. This evaluation can help guide the selection of the most effective model for practical applications in detecting defects in solar cells.

Tables from **Table 6** to **Table 13** present a comprehensive analysis of classification metrics for the top-performing models from each DL architecture family utilised in this research. The tables present metrics such as precision, recall, F1-score,

TABLE 5. Comparative analysis of dl model performance metrics across various architectures.

Model	Accuracy	Loss	Validation Accuracy	Validation Loss
SqueezeNet-1.0	0.4771	0.6940	0.4734	0.6941
SqueezeNet-1.1	0.4771	0.6940	0.4734	0.6941
VGG-11	0.8816	0.4855	0.8470	0.5081
VGG-13	0.9064	0.2637	0.8824	0.2930
VGG-16	0.4771	0.6956	0.4734	0.6958
VGG-19	0.5229	0.6925	0.5266	0.6922
ResNet-18	0.9227	0.2047	0.8986	0.2333
ResNet-34	0.9243	0.2180	0.8986	0.2574
ResNet-50	0.9244	0.2259	0.9034	0.2589
ResNet-101	0.9032	0.2520	0.8808	0.2835
ResNet-152	0.9229	0.2128	0.9002	0.2469
AlexNet	0.9280	0.2137	0.9082	0.2533
DenseNet-121	0.9512	0.1300	0.9356	0.1544
DenseNet-161	0.9168	0.2405	0.8921	0.2713
DenseNet-169	0.9572	0.1197	0.9388	0.1458
DenseNet-201	0.9353	0.1494	0.9179	0.1851
InceptionV1	0.9068	0.2607	0.8889	0.2860
InceptionV2	0.9069	0.2408	0.8824	0.2789
InceptionV3	0.9882	0.0329	0.9855	0.0416
InceptionV4	0.9134	0.1990	0.8857	0.2190
Xception	0.9929	0.0306	0.9903	0.0299
MobileNetV1	0.9942	0.0134	0.9919	0.0174
MobileNetV2	0.9995	0.0075	0.9984	0.0068
MobileNetV3	0.9050	0.2459	0.8792	0.2766

and support for both defective and non-defective classes, as well as overall metrics. **Table 6** specifically examines SqueezeNet-1.1, the most effective version of the SqueezeNet series, which demonstrates satisfactory performance with an overall F1-score of 0.32. **Table 7** displays the VGG-13 model, which is the best performance among the many versions of VGG. It achieved an overall F1-score of 0.88, indicating high precision and recall. **Table 8** showcases ResNet-152, which is considered the most prominent version of ResNet, achieving an outstanding overall F1-score of 0.90. **Table 9** provides a comprehensive breakdown of the performance of AlexNet, which attains an impressive overall F1-score of 0.91. **Table 10** displays DenseNet-169, which is considered the top-performing model in the DenseNet family. It achieves a balanced and impressive overall F1-score of 0.94. **Table 11** highlights the performance of InceptionV3, which is the best version of the Inception model. It achieves outstanding results with an overall F1-score of 0.99. **Table 12** showcases the Xception model, which consistently achieves an F1-score of 0.99 for all classes. **Table 13** showcases MobileNetV2, which demonstrates exceptional performance with an overall F1-score of 1.00, indicating its outstanding accuracy and effectiveness in detecting defects. This examination highlights the abilities of these models, emphasizing the choice of the most suitable version from each architectural family for the most effective identification of defects in solar cell images.

Figure 3 illustrates the training and validation accuracy of eight different DL models across several epochs. These models were carefully selected as the most effective variations within their respective families. Every subplot represents a distinct model. **Figure 3(a)** SqueezeNet-1.1 has a

TABLE 6. Detailed classification metrics for squeezenet-1.1 model as the best performing squeezenet variant.

Class	Precision	Recall	F1-Score	Support
Non-defective	0.47	1.00	0.64	294
Defective	0.00	0.00	0.00	327
Overall	0.24	0.50	0.32	621

TABLE 7. Detailed classification metrics for VGG-13 model as the best performing VGG variant.

Class	Precision	Recall	F1-Score	Support
Non-defective	0.80	1.00	0.89	294
Defective	1.00	0.78	0.87	327
Overall	0.90	0.89	0.88	621

TABLE 8. Detailed classification metrics for ResNet-152 model as the best performing ResNet variant.

Class	Precision	Recall	F1-Score	Support
Non-defective	0.83	1.00	0.90	294
Defective	1.00	0.81	0.90	327
Overall	0.90	0.91	0.90	621

TABLE 9. Detailed classification metrics for alexnet model.

Class	Precision	Recall	F1-Score	Support
Non-defective	0.84	1.00	0.91	294
Defective	1.00	0.83	0.90	327
Overall	0.92	0.91	0.91	621

reasonable level of accuracy, consistently hovering around 50% during the training process. This suggests that it has limits in accurately capturing the intricacies of the task.

TABLE 10. Detailed classification metrics for DenseNet-169 model as the best performing DenseNet variant.

Class	Precision	Recall	F1-Score	Support
Non-defective	0.91	0.96	0.94	294
Defective	0.96	0.92	0.94	327
Overall	0.94	0.94	0.94	621

TABLE 11. Detailed classification metrics for InceptionV3 model as the best performing inception variant.

Class	Precision	Recall	F1-Score	Support
Non-defective	0.98	0.99	0.98	294
Defective	0.99	0.98	0.99	327
Overall	0.99	0.99	0.99	621

TABLE 12. Detailed classification metrics for Xception model.

Class	Precision	Recall	F1-Score	Support
Non-defective	0.99	0.99	0.99	294
Defective	0.99	0.99	0.99	327
Overall	0.99	0.99	0.99	621

TABLE 13. Detailed classification metrics for MobileNetV2 model as the best performing MobileNet variant.

Class	Precision	Recall	F1-Score	Support
Non-defective	1.00	1.00	1.00	294
Defective	1.00	1.00	1.00	327
Overall	1.00	1.00	1.00	621

Figure 3(b) VGG-13 exhibits a significant improvement in validation accuracy, reaching around 88% within the first epoch. It then maintains a consistent performance, indicating successful learning from the dataset with minimal overfitting. **Figure 3(c)** of ResNet-152 exhibits a constant and noticeable increase in both training and validation accuracy, reaching a maximum of almost 90%. This highlights the model's capacity to effectively generalize and perform well on new, unseen data. **Figure 3(d)** demonstrates the impressive performance of AlexNet, as indicated by the rapid increase in validation accuracy to approximately 91%. This reflects the robust ability of AlexNet to extract meaningful features. **Figure 3(e)** DenseNet-169 achieves rapid and high levels of accuracy, with both training and validation measures converging at approximately 94%. This indicates that DenseNet-169 efficiently handles the propagation of features. **Figure 3(f)** InceptionV3 demonstrates outstanding performance, with a validation accuracy close to 99%. This emphasizes the efficiency of its sophisticated architecture in extracting detailed features from solar cell images. **Figure 3(g)** Xception achieves a validation accuracy close to perfection, approaching 99%, showcasing its ability to effectively handle intricate image recognition problems using its depth wise separable convolutions. **Figure 3(h)** MobileNetV2 achieves a high validation accuracy score by the second epoch, demonstrating its ideal combination of depth and processing efficiency for mobile situations. This compilation of graphs accurately depicts the learning patterns and effectiveness of cutting-edge DL models in detecting defects in solar cell images. It offers a clear visualization of the strengths and weaknesses of each model.

Figure 4 displays the training and validation loss patterns over multiple epochs for eight distinct DL models, each showcasing individual performance traits. **Figure 4(a)** demonstrates a consistent decrease in both training and validation losses for SqueezeNet-1.1. By the tenth epoch, the losses converge at approximately 0.7, suggesting moderate learning stability. However, the overall loss values remain high, indicating the potential for further improvement. **Figure 4(b)** of VGG-13 exhibits an atypical trend where the validation loss reaches its highest point abruptly during the third epoch. The graph indicates potential overfitting or instability in the model training process as a result of significant fluctuations in loss values. **Figure 4(c)** shows that ResNet-152 has a training loss that fluctuates significantly with sudden spikes. This indicates a lack of convergence and possible problems with the training data or hyperparameters. **Figure 4(d)** demonstrates that AlexNet exhibits variable loss patterns initially, but stabilizes by the fifth epoch with a significant decrease in validation loss. This suggests that the model effectively learns as the epochs go. **Figure 4(e)** shows that DenseNet-169 exhibits pronounced spikes in both training and validation losses during the initial epochs. However, these losses rapidly improve and stabilize by the tenth epoch, indicating that the model initially faced difficulties but quickly recovered and learnt effectively. **Figure 4(f)** of InceptionV3 exhibits notable variations in both training and validation losses. However, it manages to attain a low loss rate by the tenth epoch, indicating its strong ability to generalize from the training to the validation data. **Figure 4(g)** Xception exhibits consistent and small losses from the beginning, with little variation and ultimately converging towards extremely low loss values, indicating exceptional model stability and efficiency. **Figure 4(h)** MobileNetV2 demonstrates superior performance by exhibiting a significant decrease in both training and validation losses, ultimately stabilizing at a near-zero level. This emphasizes the model's outstanding capacity to successfully learn and generalize with minimum mistake. These loss trends offer crucial insights into the dependability, effectiveness, and possible difficulties encountered by each model in processing and acquiring knowledge from the dataset. This understanding is necessary for comprehending the behavior of the model in real-world scenarios.

Figure 5 displays the confusion matrices of eight DL models, offering valuable information about the performance of each model in terms of TP, FP, TN, and FN predictions for classifying flaws in solar cell images. **Figure 5(a)** SqueezeNet-1.1 fails completely in identifying any defective samples. It classifies all observations as non-defective, suggesting a notable bias or underfitting problem with the model. **Figure 5(b)** of the VGG-13 model demonstrates a significant enhancement by accurately recognizing 254 defective items. However, it falls short in recognizing 73 defective items, indicating possible areas for improving the model's sensitivity. **Figure 5(c)** shows that ResNet-152 achieves a superior equilibrium in its class predictions, with a minimal amount of incorrect negative and positive results. This

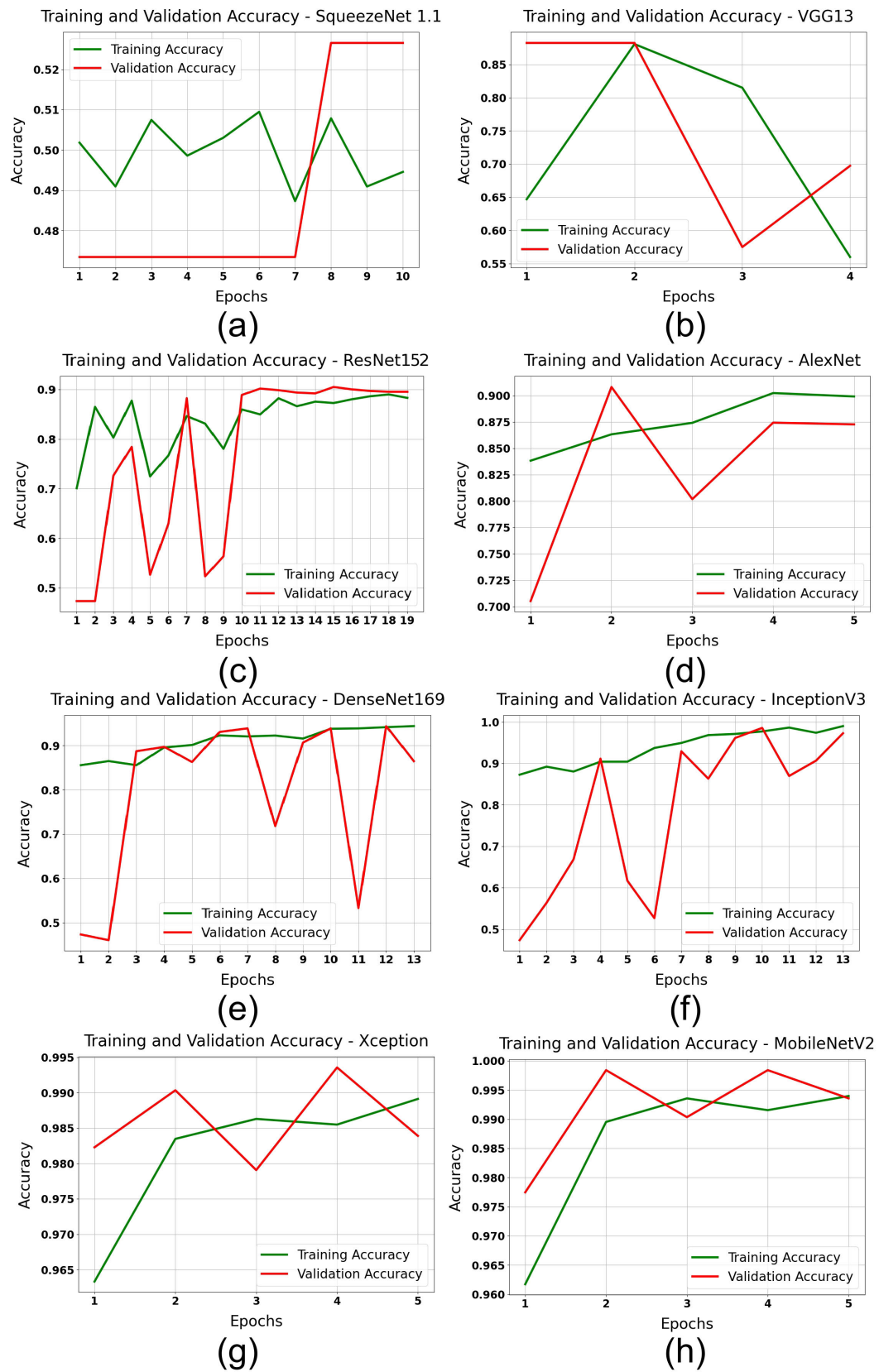


FIGURE 3. Training and Validation Accuracy for (a) SqueezeNet-1.1, (b) VGG-13, (c) ResNet-152, (d) AlexNet, (e) DenseNet-169, (f) InceptionV3, (g) Xception, and (h) MobileNetV2.

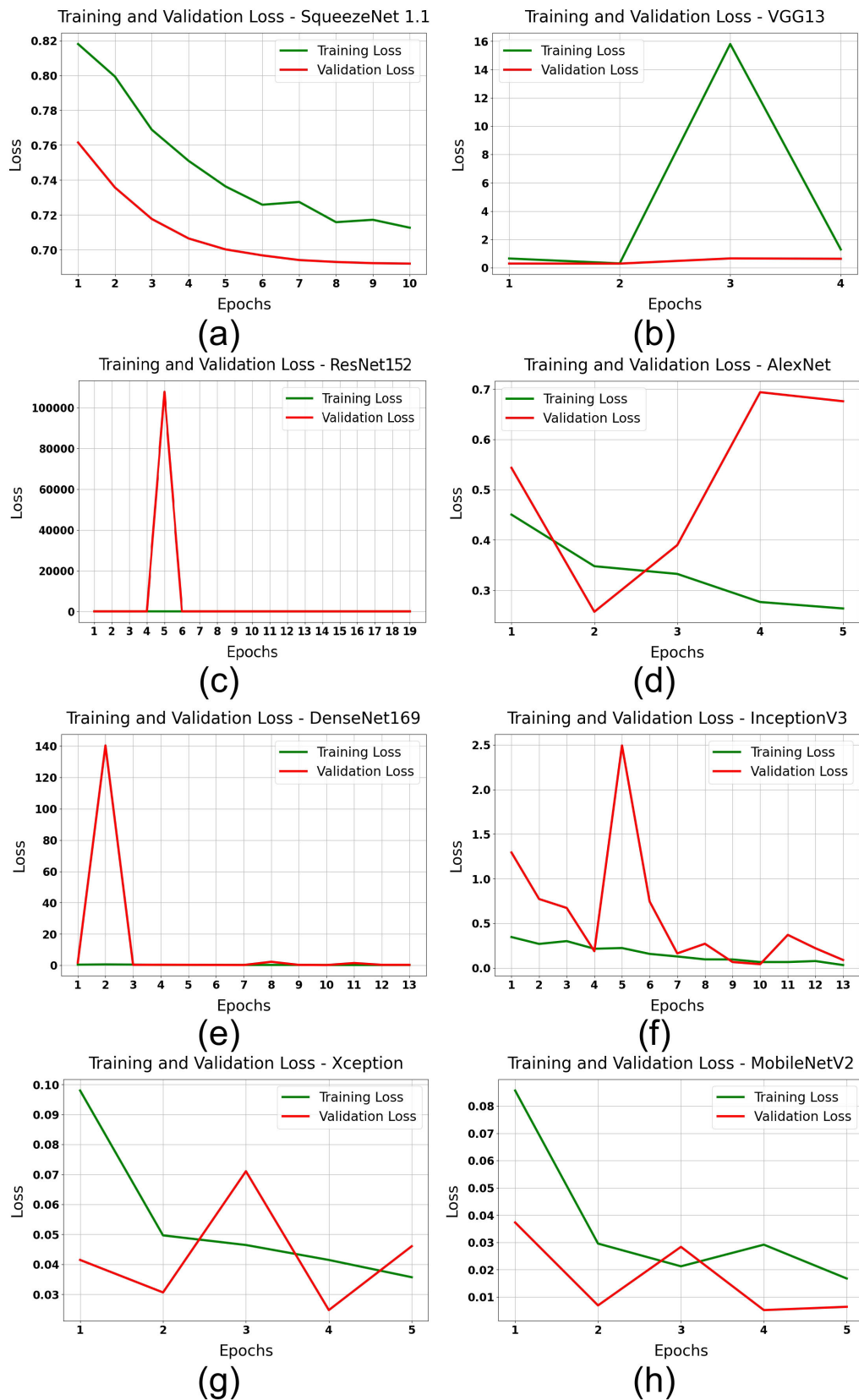


FIGURE 4. Training and Validation Loss for (a) SqueezeNet-1.1, (b) VGG-13, (c) ResNet-152, (d) AlexNet, (e) DenseNet-169, (f) InceptionV3, (g) Xception, and (h) MobileNetV2.

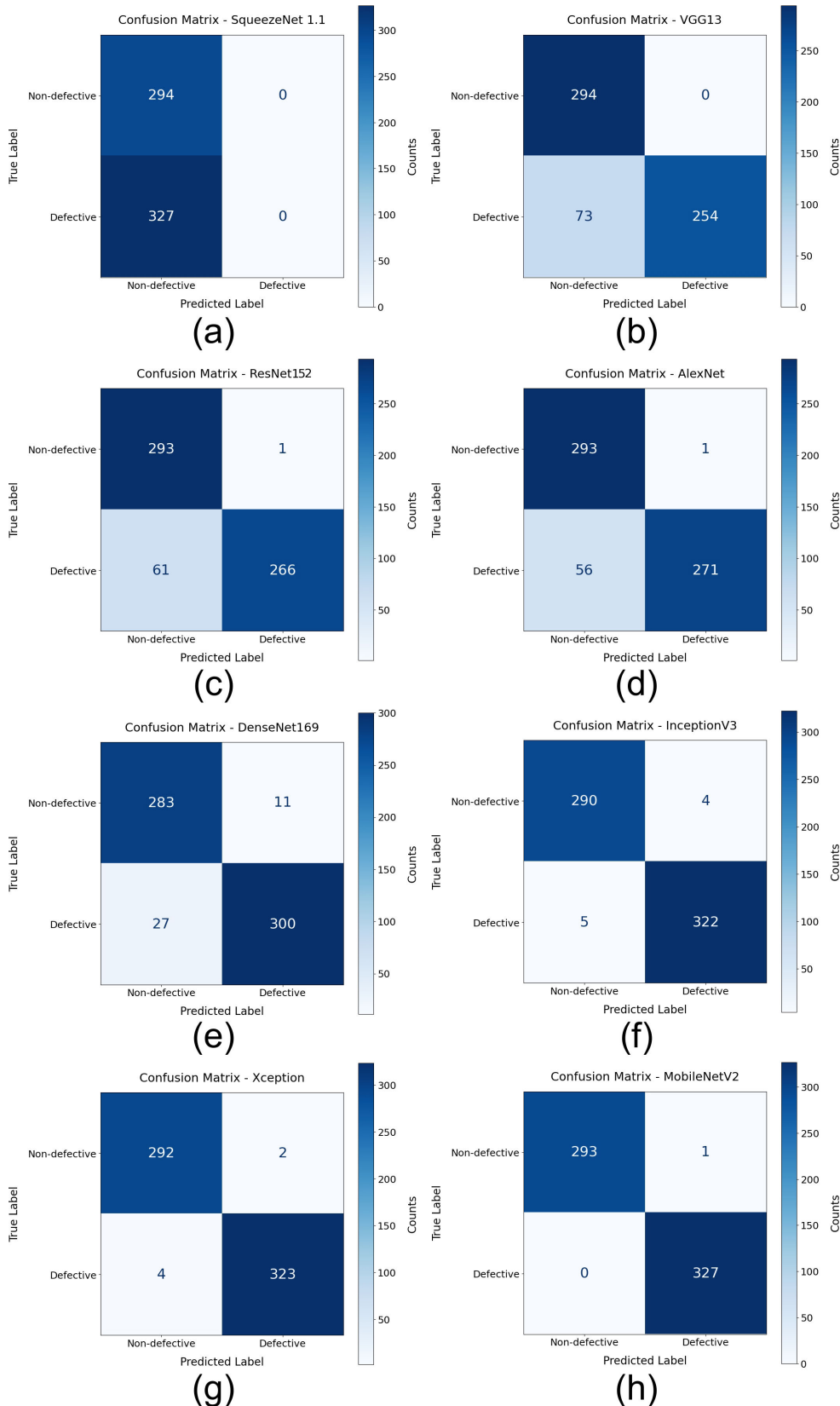


FIGURE 5. Confusion Matrix for (a) SqueezeNet-1.1, (b) VGG-13, (c) ResNet-152, (d) AlexNet, (e) DenseNet-169, (f) InceptionV3, (g) Xception, and (h) MobileNetV2.

indicates that the model has a more generalized performance. According to **Figure 5(d)**, AlexNet and ResNet-152 exhibit comparable performance, with a minimal amount of incorrect classifications. This suggests that both models are very accurate and effective in distinguishing between the different classes. **Figure 5(e)** shows that DenseNet-169 has minimal misclassifications. It correctly identifies 300 defective cases and 283 non-defective examples, indicating a strong predictive capacity with a little inclination towards finding faults. **Figure 5(f)** demonstrates that InceptionV3 achieves exceptional performance in classification, with nearly flawless accuracy. It only misclassifies a small fraction of defective and non-defective samples, indicating outstanding model training and predictive precision. **Figure 5(g)** Xception has exceptional classification performance, with only a small number of misclassifications, highlighting its resilience in dealing with intricate image classification problems. MobileNetV2 in **Figure 5(h)** demonstrates near-perfect classification, with just one non-defective sample misclassified, showcasing its remarkable model efficiency and accuracy. This study evaluated various models, categorised as high-performance, mediocre, and underperforming, using important measures such as accuracy, validation accuracy, and F1-score.

High-Performance Models:

- **MobileNetV2** stands out as the top-performing model, achieving near-perfect scores in all metrics: an accuracy of 99.95%, a validation accuracy of 99.84%, and an excellent F1-score of 99.85%. These metrics indicate that it has outstanding ability to apply knowledge to new situations, making it very successful for real-world uses where accuracy is extremely important.
- Both **Xception** and **MobileNetV1** demonstrate exceptional performance, with Xception earning almost flawless validation accuracy and loss scores, and MobileNetV1 not lagging far behind. Both models demonstrate resilience that is appropriate for intricate image classification tasks, suggesting their usefulness in critical settings such as solar panel production.

Moderate Performers:

- **DenseNet-169** and **DenseNet-121**, among other variations of DenseNet, exhibit exceptional performance with accuracy rates and F1-scores surpassing 93%. These models exhibit a favourable equilibrium between training performance and generalisation, as seen by their minimal validation losses.
- **ResNet** family models, including **ResNet-152** and **ResNet-50**, also perform well, offering a good mix of high accuracy and generalization, evidenced by their high validation accuracies and moderate validation losses.

Underperformers:

- **SqueezeNet** models and certain **VGG** variations, like as VGG-16, exhibit significantly inferior performance, with accuracies and F1-scores hovering around or falling

below 50%. These models exhibit significant losses and inadequate validation metrics, suggesting problems with either overfitting or insufficient model complexity to accurately reflect the intricacies present in the data.

- **VGG-13** stands out from the rest of its family by exhibiting significantly higher validation accuracy and F1-score. This suggests that when appropriately adjusted, VGG-13 has the ability to perform exceptionally well.

The variation in model performances can be ascribed to the changes in architecture, where models like MobileNetV2 and Xception gain advantages from recent breakthroughs in DL, such as the utilization of depth wise separable convolutions that improve learning efficiency. Conversely, more antiquated architectures such as SqueezeNet face difficulties in handling the intricacies of identifying defects in images of solar cells. The findings emphasize the significance of selecting an appropriate model that aligns with the unique attributes of the job and dataset. These insights not only assist in choosing the appropriate model, but also provide guidance for future enhancements. For example, if models are not performing well, they could potentially be improved by including advanced regularization techniques, utilizing more sophisticated data augmentation procedures, or utilizing TL from models that have demonstrated promising outcomes. By making strategic adjustments, it is possible to utilize the strengths of high-performing models to enhance the abilities of the underperforming ones, with the goal of achieving a more consistent performance overall.

Results from this study provide us with a detailed assessment of multiple DL architectures for automatic defect detection in solar cell images. In particular, MobileNetV2 obtained high accuracy of 99.95% and low validation loss at only 0.0068 which makes it a suitable model for actual applications that demand relatively good precision with very less computational cost. Xception and DenseNet-169 were both able to achieve high accuracy 99.29% and 95.72%, respectively, showing their abilities for handling complex patterns of defects. The differences in results draw a clear line of model performance: lightweight models such as MobileNet may emerge best fit for resources constrained environments while heavyweight ones like ResNet and InceptionV3 offer unsurpassed feature exploring capability at the expense higher computational complexity. This comparative examination of model performance, encompassing precision, recall, and F1-scores, offers valuable insights into the trade-offs between accuracy and efficiency. This comprehension is essential for implementing effective DL models in industrial PV systems, hence improving defect detection and quality control processes at scale.

V. CONCLUSION

This study enhances the field of automated flaw identification in solar cells by a comprehensive examination and comparison of different DL architectures. The comprehensive assessment of 24 models, encompassing both complicated

and lightweight architectures, makes a distinct and valuable contribution to the existing body of knowledge. It sheds light on the compromises between computing efficiency and detection accuracy. The results highlight the efficacy of models such as MobileNetV2 and Xception, which demonstrated high accuracy and low validation loss. These models are well-suited for implementation in industrial settings with limited computational resources. The study paper focusses on the practical consequences of implementing DL models in actual manufacturing settings. MobileNetV2 is a very efficient and powerful solution for detecting defects in real-time on the manufacturing line, thanks to its outstanding performance and low computing demands. The study also indicates that certain models, such as SqueezeNet, faced challenges in achieving high accuracy. However, models like DenseNet and Inception demonstrated a favorable combination of accuracy and processing economy. These observations can guide the choice of DL models for particular uses in the solar sector, perhaps resulting in more dependable and effective quality control systems.

VI. FUTURE WORK

Based on the discoveries made in this research, further efforts will concentrate on various crucial domains to further improve the fault identification procedure in solar cells. An immediate approach is to broaden the dataset by including a wider range of flaws. This would enhance the resilience and generalization capabilities of the models across various types of solar cells. This task will require both augmenting the quantity of images and broadening the variety of anomalies represented in the dataset, in order to ensure that the models are capable of detecting a wide spectrum of abnormalities. Another area that will receive attention is the investigation of TL and ensemble approaches. Our objective is to enhance the accuracy and dependability of defect detection by utilizing pre-trained models and integrating the advantages of diverse architectures. Moreover, the integration of these models in real-time scenarios will be a crucial advancement, specifically in fine-tuning them for edge computing devices employed in manufacturing settings. This task will need optimizing the models to achieve a harmonious equilibrium between speed, accuracy, and computing efficiency, hence ensuring their effective functioning in a production line setting. Furthermore, future studies will investigate the suitability of these models for different types of PV systems. By expanding the existing method to various categories of solar cells, Researchers can enhance the usefulness of these models and aid in the advancement of more adaptable Artificial intelligence (AI) powered quality assurance systems in the renewable energy industry. It is essential to examine how these models might be combined with current manufacturing processes, such as automated inspection systems, to fully exploit their capabilities in improving the efficiency and precision of solar cell manufacture. However, these promising results and future entities derive their innovation from built-in limitations of this study. Limitation Relatively small dataset

(although well-curated) that does not cover the full range of different types and conditions expected to appear in large PV system installations. The limitation is being addressed by expanding data collection campaigns in environmental and operational terms so that the models are more generalizable (in all types of environments) or robust. In addition, some models showed good accuracy but were computationally expensive to be deployed on low-power devices such as edge-devices. Lightweight optimization approaches, e.g., model pruning and quantization have the potential to address this issue in future research so that these competitive models can be lightweighted with computational overheads limited while maintaining their high accuracies. In conclusion, more detailed multi-class defect classification might be even useful for real-world problems in the field of PV systems and it can help to improve specific maintenance intervention activities at solar power panels.

ABBREVIATIONS

AI	Artificial Intelligence.
Adam	Adaptive Moment Estimation.
BiFPN	Bi-directional Feature Pyramid Network.
BiMAF	Bilateral Multi-Scale Adaptive Fusion.
CDPC	Cosine Distance Pseudo-Label Cross-Entropy.
CNN	Convolutional Neural Network.
CPU	Central Processing Unit.
DFB	Deep Feature-Based.
DL	Deep Learning.
DW-Conv	Depthwise Convolution.
DenseNet	Densely Connected Convolutional Network.
EL	Electroluminescence.
EdgeTPU	Edge Tensor Processing Unit.
FN	False Negative.
FP	False Positive.
FPGA	Field Programmable Gate Array.
FPN	Feature Pyramid Network.
G-SSD	Ghost Single Shot Detector.
GA-RPN	Guided Anchoring Region Proposal Network.
GAN	Generative Adversarial Network.
GD	Gradient Descent.
GSConv	Ghost Convolution.
Grad-CAM	Gradient-weighted Class Activation Mapping.
IR	Infrared Radiation.
IoU	Intersection over Union.
LwNet	Lightweight Network.
mAP	Mean Average Precision.
MCC	Matthews Correlation Coefficient.
MSFE	Multi-Scale Feature Extraction.
MobileNet	Mobile Network.
PV	Photovoltaic.
RCNN	Region-based Convolutional Neural Network.
ResNet	Residual Network.

SCT	Spatial-Channel Transformer.
SEF-CNN	Steerable Evidence Filter Convolutional Neural Network.
SENet	Squeeze-and-Excitation Network.
TL	Transfer Learning.
TLDR	Transfer Learning with Depth Reduction.
TN	True Negative.
TP	True Positive.
UAV	Unmanned Aerial Vehicle.
U-Net	U-shaped Convolutional Neural Network.
VGG	Visual Geometry Group.
VPU	Vision Processing Unit.
ViT	Vision Transformer.
YOLOX	You Only Look Once X.

REFERENCES

- [1] M. Abdelsattar, A. AbdelMoety, and A. Emad-Eldeen, “A review on detection of solar PV panels failures using image processing techniques,” in *Proc. 24th Int. Middle East Power Syst. Conf. (MEPCON)*, Mansoura, Egypt, Dec. 2023, pp. 1–6, doi: [10.1109/mepcon58725.2023.10462371](https://doi.org/10.1109/mepcon58725.2023.10462371).
- [2] M. Abdelsattar, A. M. A. E. Hamed, A. A. Elbaset, S. Kamel, and M. Ebeed, “Optimal integration of photovoltaic and shunt compensator considering irradiance and load changes,” *Comput. Electr. Eng.*, vol. 97, Jan. 2022, Art. no. 107658, doi: [10.1016/j.compeleceng.2021.107658](https://doi.org/10.1016/j.compeleceng.2021.107658).
- [3] K. Obaideen, A. G. Olabi, Y. A. Swailmeen, N. Shehata, M. A. Abdelkareem, A. H. Alami, C. Rodriguez, and E. T. Sayed, “Solar energy: Applications, trends analysis, bibliometric analysis and research contribution to sustainable development goals (SDGs),” *Sustainability*, vol. 15, no. 2, p. 1418, Jan. 2023, doi: [10.3390/su15021418](https://doi.org/10.3390/su15021418).
- [4] M. Abdelsattar, M. A. Ismeal, M. M. A. A. Zayed, A. Abdelmoety, and A. Emad-Eldeen, “Assessing machine learning approaches for photovoltaic energy prediction in sustainable energy systems,” *IEEE Access*, vol. 12, pp. 107599–107615, 2024, doi: [10.1109/ACCESS.2024.3437191](https://doi.org/10.1109/ACCESS.2024.3437191).
- [5] M. Bošnjaković, R. Santa, Z. Crnac, and T. Bošnjaković, “Environmental impact of PV power systems,” *Sustainability*, vol. 15, no. 15, p. 11888, Aug. 2023, doi: [10.3390/su15111888](https://doi.org/10.3390/su15111888).
- [6] S. Gallardo-Saavedra, L. Hernández-Callejo, M. D. C. Alonso-García, J. Muñoz-Cruzado-Alba, and J. Ballestín-Fuertes, “Infrared thermography for the detection and characterization of photovoltaic defects: Comparison between illumination and dark conditions,” *Sensors*, vol. 20, no. 16, p. 4395, Aug. 2020, doi: [10.3390/s20164395](https://doi.org/10.3390/s20164395).
- [7] A. P. Gonzalo, A. Pliego Marugán, and F. P. García Márquez, “Survey of maintenance management for photovoltaic power systems,” *Renew. Sustain. Energy Rev.*, vol. 134, Dec. 2020, Art. no. 110347, doi: [10.1016/j.rser.2020.110347](https://doi.org/10.1016/j.rser.2020.110347).
- [8] H.-H. Lin, H. K. Dandage, K.-M. Lin, Y.-T. Lin, and Y.-J. Chen, “Efficient cell segmentation from electroluminescent images of single-crystalline silicon photovoltaic modules and cell-based defect identification using deep learning with pseudo-colorization,” *Sensors*, vol. 21, no. 13, p. 4292, Jun. 2021, doi: [10.3390/s21134292](https://doi.org/10.3390/s21134292).
- [9] M. Y. Demirci, N. Besli, and A. Güümüsü, “Efficient deep feature extraction and classification for identifying defective photovoltaic module cells in electroluminescence images,” *Expert Syst. Appl.*, vol. 175, Aug. 2021, Art. no. 114810, doi: [10.1016/j.eswa.2021.114810](https://doi.org/10.1016/j.eswa.2021.114810).
- [10] A. Kaligambe and G. Fujita, “A deep learning-based framework for automatic detection of defective solar photovoltaic cells in electroluminescence images using transfer learning,” in *Proc. 4th Int. Conf. High Voltage Eng. Power Syst. (ICHVEPS)*, Aug. 2023, pp. 81–85, doi: [10.1109/ichveps58902.2023.10257399](https://doi.org/10.1109/ichveps58902.2023.10257399).
- [11] Y. Liu, J. Xu, and Y. Wu, “A CISG method for internal defect detection of solar cells in different production processes,” *IEEE Trans. Ind. Electron.*, vol. 69, no. 8, pp. 8452–8462, Aug. 2022, doi: [10.1109/TIE.2021.3104584](https://doi.org/10.1109/TIE.2021.3104584).
- [12] Y. Wang, L. Li, Y. Sun, J. Xu, Y. Jia, J. Hong, X. Hu, G. Weng, X. Luo, S. Chen, Z. Zhu, J. Chu, and H. Akiyama, “Adaptive automatic solar cell defect detection and classification based on absolute electroluminescence imaging,” *Energy*, vol. 229, Aug. 2021, Art. no. 120606, doi: [10.1016/j.energy.2021.120606](https://doi.org/10.1016/j.energy.2021.120606).
- [13] A. Bartler, L. Mauch, B. Yang, M. Reuter, and L. Stoicescu, “Automated detection of solar cell defects with deep learning,” in *Proc. 26th Eur. Signal Process. Conf. (EUSIPCO)*, Sep. 2018, pp. 2035–2039, doi: [10.2391/EUSIPCO.2018.8553025](https://doi.org/10.2391/EUSIPCO.2018.8553025).
- [14] X. Wang, “Deep learning in object recognition, detection, and segmentation,” *Found. Trends Signal Process.*, vol. 8, no. 4, pp. 217–382, 2016, doi: [10.1561/2000000071](https://doi.org/10.1561/2000000071).
- [15] M. Hassouna, M. Al-Antary, M. Saleh, and N. B. A. Barghuthi, “Applications of deep learning in medical imaging: A brief review,” in *Proc. Adv. Sci. Eng. Technol. Int. Conf. (ASET)*, Feb. 2023, pp. 1–4, doi: [10.1109/aset56582.2023.10180645](https://doi.org/10.1109/aset56582.2023.10180645).
- [16] Z. Guo, X. Li, H. Huang, N. Guo, and Q. Li, “Deep learning-based image segmentation on multimodal medical imaging,” *IEEE Trans. Radiat. Plasma Med. Sci.*, vol. 3, no. 2, pp. 162–169, Mar. 2019, doi: [10.1109/TRPMS.2018.2890359](https://doi.org/10.1109/TRPMS.2018.2890359).
- [17] R. S. Pahwa, R. Chang, W. Jie, X. Xun, O. Z. Min, F. C. Sheng, C. S. Choong, and V. S. Rao, “Automated detection and segmentation of HBMs in 3D X-ray images using semi-supervised deep learning,” in *Proc. IEEE 72nd Electron. Compon. Technol. Conf. (ECTC)*, May 2022, pp. 1890–1897, doi: [10.1109/ECTC51906.2022.00297](https://doi.org/10.1109/ECTC51906.2022.00297).
- [18] M. Abdelsattar, A. A. A. Rasslan, and A. Emad-Eldeen, “Detecting dusty and clean photovoltaic surfaces using MobileNet variants for image classification,” *SVU-Int. J. Eng. Sci. Appl.*, vol. 6, no. 1, pp. 9–18, Jun. 2025.
- [19] E. S. Oda, M. Ebeed, A. M. A. E. Hamed, A. Ali, A. A. Elbaset, and M. Abdelsattar, “Optimal allocation of a hybrid photovoltaic-based DG and DSTATCOM under the load and irradiance variability,” *Int. Trans. Electr. Energy Syst.*, vol. 31, no. 11, p. 13131, Nov. 2021, doi: [10.1002/2050-7038.13131](https://doi.org/10.1002/2050-7038.13131).
- [20] A. A. Elbaset, H. Ali, and M. A. E. Sattar, “Design and performance of single-phase grid inverter photovoltaic system for residential applications with maximum power point tracking,” in *Proc. 18th Int. Middle East Power Syst. Conf. (MEPCON)*, Cairo, Egypt, Dec. 2016, pp. 266–275, doi: [10.1109/MEPCON.2016.7836901](https://doi.org/10.1109/MEPCON.2016.7836901).
- [21] A. F. Abulkhair, M. Abdelsattar, and H. A. Mohamed, “Negative effects and processing methods review of renewable energy sources on modern power system: A review,” *Int. J. Renew. Energy Res.*, vol. 14, no. 2, pp. 385–394, 2024, doi: [10.20508/ijrer.v14i2.14346.g8898](https://doi.org/10.20508/ijrer.v14i2.14346.g8898).
- [22] M. Abdelsattar, M. A. Ismeal, M. M. Aly, and S. S. Abu-Elwafa, “Energy management of microgrid with renewable energy sources: A case study in hurghada Egypt,” *IEEE Access*, vol. 12, pp. 19500–19509, 2024, doi: [10.1109/ACCESS.2024.3356556](https://doi.org/10.1109/ACCESS.2024.3356556).
- [23] W. Zhang, V. Archana, O. Gandhi, C. D. Rodríguez-Gallegos, H. Quan, D. Yang, C.-W. Tan, C. Y. Chung, and D. Srinivasan, “SoilingEdge: PV soiling power loss estimation at the edge using surveillance cameras,” *IEEE Trans. Sustain. Energy*, vol. 15, no. 1, pp. 556–566, Jan. 2024, doi: [10.1109/TSTE.2023.3320690](https://doi.org/10.1109/TSTE.2023.3320690).
- [24] S. Hao, T. He, X. Ma, X. Zhang, Y. Wu, and H. Wang, “KDBIDet: A bi-branch collaborative training algorithm based on knowledge distillation for photovoltaic hot-spot detection systems,” *IEEE Trans. Instrum. Meas.*, vol. 73, pp. 1–15, 2024, doi: [10.1109/TIM.2023.3335509](https://doi.org/10.1109/TIM.2023.3335509).
- [25] E. A. Ramadan, N. M. Moawad, B. A. Abouzalm, A. A. Sakr, W. F. Abouzaid, and G. M. El-Banby, “An innovative transformer neural network for fault detection and classification for photovoltaic modules,” *Energy Convers. Manage.*, vol. 314, Aug. 2024, Art. no. 118718, doi: [10.1016/j.enconman.2024.118718](https://doi.org/10.1016/j.enconman.2024.118718).
- [26] X. Chao, L. Zhang, Y. Li, C. Huang, and J. Li, “Photovoltaic fault detection based on infrared and visible image augmentation and fusion,” *Turkish J. Agricult. Forestry*, vol. 48, no. 3, pp. 430–442, Jun. 2024, doi: [10.55730/1300-011x.3192](https://doi.org/10.55730/1300-011x.3192).
- [27] H. M. Al-Otum, “Classification of anomalies in electroluminescence images of solar PV modules using CNN-based deep learning,” *Sol. Energy*, vol. 278, Aug. 2024, Art. no. 112803, doi: [10.1016/j.solener.2024.112803](https://doi.org/10.1016/j.solener.2024.112803).
- [28] R. Tang, Z. Ren, S. Ning, and Y. Zhang, “Fault classification of photovoltaic module infrared images based on transfer learning and interpretable convolutional neural network,” *Sol. Energy*, vol. 276, Jul. 2024, Art. no. 112703, doi: [10.1016/j.solener.2024.112703](https://doi.org/10.1016/j.solener.2024.112703).
- [29] X. Zhang, Y. Ge, Y. Wang, J. Wang, W. Wang, and L. Lu, “Residual learning-based robotic image analysis model for low-voltage distributed photovoltaic fault identification and positioning,” *Frontiers Neurorobotics*, vol. 18, Apr. 2024, Art. no. 1396979, doi: [10.3389/fnbot.2024.1396979](https://doi.org/10.3389/fnbot.2024.1396979).
- [30] X. Hu, Z. Du, and F. Wang, “Research on detection method of photovoltaic cell surface dirt based on image processing technology,” *Sci. Rep.*, vol. 14, no. 1, p. 16842, Jul. 2024, doi: [10.1038/s41598-024-68052-z](https://doi.org/10.1038/s41598-024-68052-z).

- [31] Y. Cao, D. Pang, Q. Zhao, Y. Yan, Y. Jiang, C. Tian, F. Wang, and J. Li, "Improved YOLOv8-GD deep learning model for defect detection in electroluminescence images of solar photovoltaic modules," *Eng. Appl. Artif. Intell.*, vol. 131, May 2024, Art. no. 107866, doi: [10.1016/j.engappai.2024.107866](https://doi.org/10.1016/j.engappai.2024.107866).
- [32] Q. Liu, M. Liu, C. Wang, and Q. M. J. Wu, "An efficient CNN-based detector for photovoltaic module cells defect detection in electroluminescence images," *Sol. Energy*, vol. 267, Jan. 2024, Art. no. 112245, doi: [10.1016/j.solener.2023.112245](https://doi.org/10.1016/j.solener.2023.112245).
- [33] Y. S. Balcioglu, B. Sezen, and C. C. Cerasi, "Solar cell busbars surface defect detection based on deep convolutional neural network," *IEEE Latin Amer. Trans.*, vol. 21, no. 2, pp. 242–250, Feb. 2023, doi: [10.1109/LTA.2023.10015216](https://doi.org/10.1109/LTA.2023.10015216).
- [34] M. Xu, "Solar cell defect detection based on improved G-SSD network," *Int. J. Energy*, vol. 2, no. 1, pp. 68–71, Mar. 2023, doi: [10.5409/ije.v2i1.5618](https://doi.org/10.5409/ije.v2i1.5618).
- [35] L. Zhang, Y. Bian, P. Jiang, and F. Zhang, "A transfer residual neural network based on ResNet-50 for detection of steel surface defects," *Appl. Sci.*, vol. 13, no. 9, p. 5260, Apr. 2023, doi: [10.3390/app13095260](https://doi.org/10.3390/app13095260).
- [36] P. Arafin, A. M. Billah, and A. Issa, "Deep learning-based concrete defects classification and detection using semantic segmentation," *Struct. Health Monitor.*, vol. 23, no. 1, pp. 383–409, Jan. 2024, doi: [10.1177/14759217231168212](https://doi.org/10.1177/14759217231168212).
- [37] S. Jumaboev, D. Jurakuziev, and M. Lee, "Photovoltaics plant fault detection using deep learning techniques," *Remote Sens.*, vol. 14, no. 15, p. 3728, Aug. 2022, doi: [10.3390/rs14153728](https://doi.org/10.3390/rs14153728).
- [38] J. Wang, L. Bi, P. Sun, X. Jiao, X. Ma, X. Lei, and Y. Luo, "Deep-learning-based automatic detection of photovoltaic cell defects in electroluminescence images," *Sensors*, vol. 23, no. 1, p. 297, Dec. 2022, doi: [10.3390/s23010297](https://doi.org/10.3390/s23010297).
- [39] H. Tellal, M. Mohandes, B. Liu, S. Rehman, and A. Al-Shaikh, "Deep learning system for defect classification of solar panel cells," in *Proc. 14th Int. Conf. Comput. Intell. Commun. Netw. (CICN)*, Dec. 2022, pp. 448–453, doi: [10.1109/CICN56167.2022.10008277](https://doi.org/10.1109/CICN56167.2022.10008277).
- [40] A. S. Al-Waisy, D. A. Ibrahim, D. A. Zebari, S. Hammadi, H. Mohammed, M. A. Mohammed, and R. Damaševičius, "Identifying defective solar cells in electroluminescence images using deep feature representations," *PeerJ Comput. Sci.*, vol. 8, p. e992, May 2022, doi: [10.7717/peerj.cs.992](https://doi.org/10.7717/peerj.cs.992).
- [41] A. Katiyar, S. Behal, and J. Singh, "Automated defect detection in physical components using machine learning," in *Proc. 8th Int. Conf. Comput. Sustain. Global Develop. (INDIACom)*, Mar. 2021, pp. 527–532.
- [42] I. Zyout and A. Oatawneh, "Detection of PV solar panel surface defects using transfer learning of the deep convolutional neural networks," in *Proc. Adv. Sci. Eng. Technol. Int. Conf. (ASET)*, Feb. 2020, pp. 1–4, doi: [10.1109/ASET48392.2020.9118382](https://doi.org/10.1109/ASET48392.2020.9118382).
- [43] B. Su, H. Chen, P. Chen, G. Bian, K. Liu, and W. Liu, "Deep learning-based solar-cell manufacturing defect detection with complementary attention network," *IEEE Trans. Ind. Informat.*, vol. 17, no. 6, pp. 4084–4095, Jun. 2021, doi: [10.1109/TII.2020.3008021](https://doi.org/10.1109/TII.2020.3008021).
- [44] X. Li, Q. Yang, Z. Lou, and W. Yan, "Deep learning based module defect analysis for large-scale photovoltaic farms," *IEEE Trans. Energy Convers.*, vol. 34, no. 1, pp. 520–529, Mar. 2019, doi: [10.1109/TEC.2018.2873358](https://doi.org/10.1109/TEC.2018.2873358).
- [45] L. Liu, Y. Zhu, M. R. Ur Rahman, P. Zhao, and H. Chen, "Surface defect detection of solar cells based on feature pyramid network and GA-faster-RCNN," in *Proc. 2nd China Symp. Cognit. Comput. Hybrid Intell. (CCHI)*, Sep. 2019, pp. 292–297, doi: [10.1109/CCHI.2019.8901952](https://doi.org/10.1109/CCHI.2019.8901952).
- [46] H. Chen, S. Wang, and J. Xing, "Detection of cracks in electroluminescence images by fusing deep learning and structural decoupling," in *Proc. Chin. Autom. Congr. (CAC)*, Nov. 2019, pp. 2565–2569, doi: [10.1109/CAC4863.2019.8996338](https://doi.org/10.1109/CAC4863.2019.8996338).
- [47] M. R. U. Rahman, H. Chen, and W. X. Xi, "U-net based defects inspection in photovoltaic electroluminescence images," in *Proc. IEEE Int. Conf. Big Knowl. (ICBK)*, Nov. 2019, pp. 215–220, doi: [10.1109/ICBK.2019.00036](https://doi.org/10.1109/ICBK.2019.00036).
- [48] C. Buerhop-Lutz, S. Deitsch, A. Maier, F. Gallwitz, S. Berger, B. Doll, J. Hauch, C. Camus, and C. J. Brabec, "A benchmark for visual identification of defective solar cells in electroluminescence imagery," in *Proc. Eur. PV Sol. Energy Conf. Exhib. (EUPVSEC)*, 2018, pp. 1287–1289, doi: [10.4229/35thEUPVSEC2018-5CV.3.15](https://doi.org/10.4229/35thEUPVSEC2018-5CV.3.15).
- [49] S. Deitsch, C. Buerhop-Lutz, E. Sovetkin, A. Steland, A. Maier, F. Gallwitz, and C. Riess, "Segmentation of photovoltaic module cells in uncalibrated electroluminescence images," *Mach. Vis. Appl.*, vol. 32, no. 4, p. 84, Jul. 2021, doi: [10.1007/s00138-021-01191-9](https://doi.org/10.1007/s00138-021-01191-9).
- [50] S. Deitsch, V. Christlein, S. Berger, C. Buerhop-Lutz, A. Maier, F. Gallwitz, and C. Riess, "Automatic classification of defective photovoltaic module cells in electroluminescence images," *Sol. Energy*, vol. 185, pp. 455–468, Jun. 2019, doi: [10.1016/j.solener.2019.02.067](https://doi.org/10.1016/j.solener.2019.02.067).
- [51] K. He, X. Zhang, S. Ren, and J. Sun, "Deep residual learning for image recognition," in *Proc. IEEE Conf. Comput. Vis. Pattern Recognit. (CVPR)*, Jun. 2016, pp. 770–778, doi: [10.1109/CVPR.2016.90](https://doi.org/10.1109/CVPR.2016.90).
- [52] G. Huang, Z. Liu, L. Van Der Maaten, and K. Q. Weinberger, "Densely connected convolutional networks," in *Proc. IEEE Conf. Comput. Vis. Pattern Recognit. (CVPR)*, Jul. 2017, pp. 2261–2269, doi: [10.1109/CVPR.2017.243](https://doi.org/10.1109/CVPR.2017.243).
- [53] O. Russakovsky, J. Deng, H. Su, J. Krause, S. Satheesh, S. Ma, Z. Huang, A. Karpathy, A. Khosla, M. Bernstein, A. C. Berg, and L. Fei-Fei, "ImageNet large scale visual recognition challenge," *Int. J. Comput. Vis.*, vol. 115, no. 3, pp. 211–252, Dec. 2015, doi: [10.1007/s11263-015-0816-y](https://doi.org/10.1007/s11263-015-0816-y).
- [54] S. Liu and W. Deng, "Very deep convolutional neural network based image classification using small training sample size," in *Proc. 3rd IAPR Asian Conf. Pattern Recognit. (ACPR)*, Nov. 2015, pp. 730–734, doi: [10.1109/ACPR.2015.7486599](https://doi.org/10.1109/ACPR.2015.7486599).
- [55] C. Szegedy, V. Vanhoucke, S. Ioffe, J. Shlens, and Z. Wojna, "Rethinking the inception architecture for computer vision," in *Proc. IEEE Conf. Comput. Vis. Pattern Recognit. (CVPR)*, Jun. 2016, pp. 2818–2826, doi: [10.1109/CVPR.2016.308](https://doi.org/10.1109/CVPR.2016.308).
- [56] M. Sandler, A. Howard, M. Zhu, A. Zhmoginov, and L.-C. Chen, "MobileNetV2: Inverted residuals and linear bottlenecks," in *Proc. IEEE/CVF Conf. Comput. Vis. Pattern Recognit.*, Jun. 2018, pp. 4510–4520, doi: [10.1109/CVPR.2018.00474](https://doi.org/10.1109/CVPR.2018.00474).
- [57] F. Chollet, "Xception: Deep learning with depthwise separable convolutions," in *Proc. IEEE Conf. Comput. Vis. Pattern Recognit. (CVPR)*, Jul. 2017, pp. 1800–1807, doi: [10.1109/CVPR.2017.195](https://doi.org/10.1109/CVPR.2017.195).
- [58] F. M. Siraj, S. T. K. Ayon, M. A. Samad, J. Uddin, and K. Choi, "Few-shot lightweight SqueezeNet architecture for induction motor fault diagnosis using limited thermal image dataset," *IEEE Access*, vol. 12, pp. 50986–50997, 2024, doi: [10.1109/ACCESS.2024.3385430](https://doi.org/10.1109/ACCESS.2024.3385430).
- [59] R. Yacoubi and D. Axman, "Probabilistic extension of precision, recall, and F1 score for more thorough evaluation of classification models," in *Proc. 1st Workshop Eval. Comparison NLP Syst.*, 2020, pp. 79–91, doi: [10.18653/v1/2020.eval4nlp-1.9](https://doi.org/10.18653/v1/2020.eval4nlp-1.9).
- [60] M. Owusu-Adjei, J. B. Hayfron-Acquah, T. Frimpong, and G. Abdul-Salaam, "Imbalanced class distribution and performance evaluation metrics: A systematic review of prediction accuracy for determining model performance in healthcare systems," *PLOS Digit. Health*, vol. 2, no. 11, Nov. 2023, Art. no. e0000290, doi: [10.1371/journal.pdig.0000290](https://doi.org/10.1371/journal.pdig.0000290).
- [61] W. Siblini, J. Fréry, L. He-Guelton, F. Oblé, and Y. Wang, "Master your metrics with calibration," in *Advances in Intelligent Data Analysis XVIII*, M. R. Berthold et al., Eds., Cham, Switzerland: Springer, 2020, pp. 457–469, doi: [10.1007/978-3-030-44584-3_36](https://doi.org/10.1007/978-3-030-44584-3_36). [Online]. Available: https://link.springer.com/chapter/10.1007/978-3-030-44584-3_36#citeas
- [62] A. Emad-Eldeen, M. A. Azim, M. Abdelsattar, and A. AbdelMoety, "Utilizing machine learning and deep learning for enhanced supercapacitor performance prediction," *J. Energy Storage*, vol. 100, Oct. 2024, Art. no. 113556, doi: [10.1016/j.est.2024.113556](https://doi.org/10.1016/j.est.2024.113556).



MONTASER ABDELSATTAR was born in Abu-Tisht, Qena, Egypt, in August 1983. He received the B.Sc. degree from the Electrical Engineering Department, Faculty of Engineering, Al-Azhar University, Egypt, in 2006, and the M.Sc. and Ph.D. degrees in electrical engineering from the Faculty of Engineering, Minia University, Egypt, in 2011 and 2015, respectively. He was a Lecturer with the Department of Electrical and Computer Engineering, El-Minia High Institute of Engineering and Technology, El-Minia, Egypt, from October 2016 to October 2020. He was also a Lecturer with the Electrical Engineering Department,

Faculty of Engineering, South Valley University, Qena, from November 2020 to September 2021, where he has been an Associate Professor and the Head of the Electrical Engineering Department, Faculty of Engineering, since October 2021. His current research interests include renewable energy sources, energy management, artificial intelligence, machine learning techniques, smart grid, micro-grid, power quality, power systems, control, electric vehicles, and optimization algorithms. He has published over 60 technical papers in international journals and conferences and has supervised and examined more than ten M.Sc. and Ph.D. theses with South Valley University, Minia University, Sohag University, Aswan University, and other Egyptian universities. He has published three international books in the field of renewable energy.



MOHAMED A. ISMEIL (Senior Member, IEEE) was born in Qena, Egypt, in October 1977. He received the B.Sc. and M.Sc. degrees in electrical engineering from South Valley University, in 2002 and 2008, respectively, and the Ph.D. degree from Aswan University, in April 2014. From October 2010 to January 2013, he was a Ph.D. Student with the Department of Electrical Drive Systems and Power Electronics, Technical University of Munich (TUM), Germany, as the Channel System Program. From April 2014 to September 2018, he was an Assistant Professor with the Aswan Faculty of Engineering, Aswan University, and since October 2018, he has been an Associate Professor with the Qena Faculty of Engineering, South Valley University. From March 2020 to November 2022, he was the Head of the Electrical Department, Qena Faculty of Engineering. Since November 2002, he has been an Associate Professor with the College of Engineering, King Khalid University, Saudi Arabia. He has published more than 78 papers in international conferences and journals. His current research interests include power electronics applications in wind energy conversion systems, PV interface with the utility, smart grid technologies, digital control applications (PIC, FPGA, and DSP), and power inverter design for renewable applications.



AHMED EMAD-ELDEEN was born in Egypt, in September 1982. He received the bachelor's degree in electronics technology, the master's degree in electronics technology, and the Ph.D. degree in renewable energy science and engineering from Beni-Suef University, Beni Suef, Egypt, in 2007, 2014, and 2020, respectively. He has specialized in the field of renewable energy science and engineering. Beginning his career with Beni-Suef University, in 2009, he initially was a Demonstrator in electronics technology. His commitment and passion for teaching and research led to his subsequent roles as an Assistant Lecturer and then as a Lecturer in renewable energy science and engineering. Currently, he holds the position of a Lecturer with the Faculty of Postgraduate Studies for Advanced Sciences, Beni-Suef University. His work focuses on renewable energy education and pioneering research in the field, contributing to the advancement of sustainable and eco-friendly energy solutions.



AHMED ABDELMOETY was born in Amman, Jordan, in February 1999. He received the Bachelor of Science degree in electrical power and machinery engineering from South Valley University, Qena, Egypt, in 2022, where he is currently pursuing the Master of Science degree in electrical engineering. His research interests include renewable energy sources, AI, machine learning, and deep learning, aiming to advance smart energy solutions.

• • •